eprints@whiterose.ac.uk
https://eprints.whiterose.ac.uk/

Transfer of Complex Regional Pain Syndrome to mice via human autoantibodies is mediated by interleukin-1-induced mechanisms

Z. Helyes[1,4,#§], V. Tékus[1#], N. Szentes[1#], K. Pohóczky[1,9], B. Botz[1], T. Kiss[1], Á Kemény[1], Z. Környei[2], K. Tóth[2], N. Lénárt[2], H. Ábrahám[3], E. Pinteaux [5], S. Francis[6], S. Sensi[7], Á. Dénes[2§] and A. Goebel[7,8§]

[1]Department of Pharmacology and Pharmacotherapy, Medical School; János Szentágothai Research Centre & Centre for Neuroscience, University of Pécs, Pécs, Hungary

[2]Momentum Laboratory of Neuroimmunology, Institute of Experimental Medicine, Budapest, Hungary

[3]Department of Biology and Electron Microscopy, Medical School, University of Pécs, Pécs, Hungary

[4]PharmInVivo Ltd., Pécs, Hungary

[5]Division of Neuroscience and Experimental Neurology, Faculty of Biology, Medicine, and Health. University of Manchester, Manchester, UK.

[6]Department of Infection, Immunity and Cardiovascular Disease, University of Sheffield, Sheffield, UK.

[7]Department of Translational Medicine, University of Liverpool, Liverpool, UK

[8]The Walton Centre NHS Foundation Trust, Liverpool, UK

[9]Department of Pharmacology, Faculty of Pharmacy, University of Pécs, Pécs, Hungary

#Zs. Helyes, V. Tékus and N. Szentes made equal contributions to the present work.

§A. Goebel, Zs. Helyes and A. Denes are indicated as equal corresponding authors in this paper.

Clinical work, IgG preparation: A. Goebel, Pain Research Institute, Department of Translational Medicine, University of Liverpool, Liverpool L7 7AL, UK. Tel.: +44 151 529 5820; fax: +44 151 529 5821; e-mail: andreasgoebel@rocketmail.com, andreas.goebel@liv.ac.uk

Animal experiments: Zs Helyes, University of Pécs Medical School, Department of Pharmacology and Pharmacotherapy & Szentagothai Research Centre. Tel: +36 72 5202802; fax: +36 72 536218; e-mail: zsuzsanna.helyes@aok.pte.hu

IL-1 gene-deleted mice and neuroinflammation: A. Denes; Momentum Laboratory of Neuroimmunology, Institute of Experimental Medicine, Budapest, Hungary. Tel:+36209549149; e-mail: denesa@koki.hu

Abstract

Neuro-immune interactions may contribute to severe pain, and regional inflammatory and autonomic signs in Complex Regional Pain Syndrome (CRPS). However, the pathophysiological mechanisms remain unclear and therapies are unsatisfactory. Here we investigated peripheral and central immune mechanisms in a passive transfer-trauma translational mouse model of CRPS, where small plantar skin-muscle incision was performed in female C57Bl/6 mice treated daily with purified serum-IgG from patients with longstanding CRPS, or healthy volunteers. CRPS IgG significantly increased and prolonged swelling, and induced stable hyperalgesia of the incised paw compared to IgG from healthy patients. Following a short-lasting paw inflammatory response in all groups, CRPS mice displayed sustained microglia and astrocyte activation in the dorsal horn of the spinal cord and in pain-related brain regions, indicating central sensitization. Genetic deletion of interleukin-1 (IL-1) using IL-1αβ KO mice and perioperative IL-1 receptor type 1 (IL-1R1) blockade with the drug anakinra, but not steroid treatment precluded the development of transferred CRPS. Anakinra treatment also abrogated the established sensitization phenotype when initiated 8 days after incision. Furthermore, with the generation of a novel IL-1β$^{fl/fl}$ mouse line, we demonstrated that these actions are in part mediated by microglia-derived IL-1β, suggesting that both peripheral and central inflammatory mechanisms contribute to the transferred CRPS phenotype. These results indicate that persistent CRPS is mediated by autoantibodies and highlight a novel therapeutic use for clinically licensed antagonists, such as anakinra, to prevent or treat CRPS via blocking IL-1 actions.

Significance statement: Severe chronic pain is a common health problem, which can profoundly affect the quality of life for patients. Currently, the mechanisms of chronic pain are not completely understood and there are few pain-relieving drug treatments that are effective long-term. In this study we show that serum autoantibodies from patients with a severe, posttraumatic chronic pain condition, but not serum autoantibodies from healthy controls, cause long-lasting unilateral paw hypersensitivity in mice after acute hind-paw injury, mimicking the clinical condition. These symptoms can be prevented by blocking the actions of the proinflammatory mediator, interleukin-1 (IL-1) with the drug anakinra, which is licensed for clinical use. Our findings show that antibody-mediated autoimmunity contributes to the

development of severe chronic pain after injury and that blockade of IL-1 actions is therapeutically effective.

INTRODUCTION

Complex Regional Pain Syndrome (CRPS), with a prevalence of about 1:2000, is a severe chronic pain experienced by humans. CRPS is usually triggered by trauma to the distal regions of a limb, and is further associated with limb-restricted sensory, motor, autonomic, and trophic abnormalities, and profound sensory central nervous system (CNS) reorganisation. In CRPS no or only minimal tissue destruction occurs (1, 2). The pathophysiological mechanisms underlying CRPS are poorly understood. Systemic inflammatory markers remain normal in CRPS patients, but regional inflammatory mediators and autoimmunity are suggested to contribute to the manifestation of the symptoms (1, 3). Furthermore, neuro-plasticity mechanisms within the spinal cord and the brain are believed to sustain persistent pain and associated cognitive and emotional changes (2, 4, 5).

While most patients with CRPS show an improvement within months, either with or without treatment (6), 1 in 5 patients develop persistent pain, often lasting years or even through their lifetime (7). This type of persistent pain is intrusive and results in amongst the lowest quality of life scores in medical conditions (8). Among the few drug trials performed to date (9) neither conventional drugs used to relieve pain, such as non-steroidal anti-inflammatory drugs, opioids, anti-depressants, or anti-epileptics (10), nor steroids (11, 12) have shown significant efficacy in persistent CRPS. Implantation of a spinal cord stimulator, which delivers electrical impulses to the dorsal column can over-ride CRPS pain in about 50% of the patients (13), but the duration of the optimum effect is limited to a few years (14). Since many patients cannot be successfully treated (7, 15), the treatment of CRPS remains an important unresolved problem and is still an unmet medical need (16). Thus, to better understand the peripheral and central pathophysiological mechanisms underlying CRPS, reliable and validated animal models are desperately needed (16, 17).

We have recently shown that passive transfer of serum-IgG from CRPS patients to hindpaw-injured rodents elicits key features (unilateral hyperalgesia and edema) of the clinical condition

(18). This suggests a 2-hit pathology, where circulating IgG autoantibodies are rendered pathogenic in the context of paw injury-related regional or central modifications (3). Although these behavioural results indicated that serum IgG autoantibodies contribute to the disease pathophysiology, and thus provided the first evidence for the construct-validity of the transfer model, the observed abnormalities were modest-sized and short-lasting, and the mechanisms mediating them remain unknown.

Using samples available from patients who consented to repeat donation of larger blood volumes, or who had received plasma exchange treatment (19, 20), we have now developed an enhanced passive IgG transfer-trauma model, and have examined its translational validity. We investigated, i) whether and how transferred behavioural signs are augmented and sustained to resemble the clinical phenotype, and whether there are differences between preparations from different patients, ii) the degree of regional post-traumatic immune activation in the paw, given that mild, transient immune activation in the affected skin is sometimes detected in patients (21), and its correlation to behavioural parameters, iii) the degree and mechanisms of post-traumatic glial activation in the spinal cord since strong CNS re-organisation is recognized in the clinical cases (4, 22), and finally iv) whether targeting specific inflammatory pathways at the time of, or after trauma can prevent or treat transferred CRPS (tCRPS) to provide a translatable therapeutic approach.

RESULTS

Daily administration of serum IgG from CRPS patients induces profound and persistent post-incisional mechanical hyperalgesia.

The pre-operation mechanonociceptive threshold values of the affected limbs were 8.65 $\pm$ 0.08, 8.69 $\pm$ 0.09 and 8.60 $\pm$ 0.07 in the saline, healthy IgG- and CRPS IgG-treated mice, respectively (not significantly different, Fig. 1A). Plantar skin and muscle incision induced a 45-50 % relative decrease of the mechanonociceptive threshold in all groups 1 day after the surgery. Upon daily injections, paw sensitivity quickly recovered to mild hyperalgesia in both saline and healthy IgG injected animals, with mild, non-significantly enhanced values remaining in the healthy IgG group versus the saline group throughout the experimental period. Injection of IgG from CRPS patients caused significantly augmented hyperalgesia compared to IgG from healthy volunteers, which appeared to be further enhanced towards the end of the experimental period. This effect was evident in the IgG preparations from each individually tested patient (n=7), as well as a preparation pooled from 7 separate patients (Fig. 2, supplementary appendix Fig. S2). The observed 15-32% absolute threshold reduction was two-fold compared to that seen in our previously published experimental model (injections on day -1, 0, 5, 6) (18). Contralateral paws retained normal sensitivity in all groups (supplementary appendix Fig.S1). Post-surgical weight loss compared with baseline reached a nadir at days 3-4, and the weights of the animal then fully recovered, without significant differences between groups (supplementary appendix Fig. S0). We observed no spontaneous nocifensive behaviours, such as paw biting, lifting, licking.

In all groups, injured paws developed about 30% relative paw swelling (defined as edema) on day 1, but there were no changes in contralateral paws (supplementary appendix Fig. S1). Edema resolved in healthy IgG and saline groups, but CRPS IgG injection significantly slowed edema resolution (Fig. 1B). Whereas the pattern of transferred hyperalgesia was uniform, there was important variability in the degree and pattern of transferred swelling between different patient preparations, with no correlation between these two parameters (Fig. 2, supplementary appendix Figs. S2-3). Minimal weight loss was observed with a nadir on days 3-4 post surgery and no difference between injection groups (supplementary appendix Fig. S0).

Figure 1
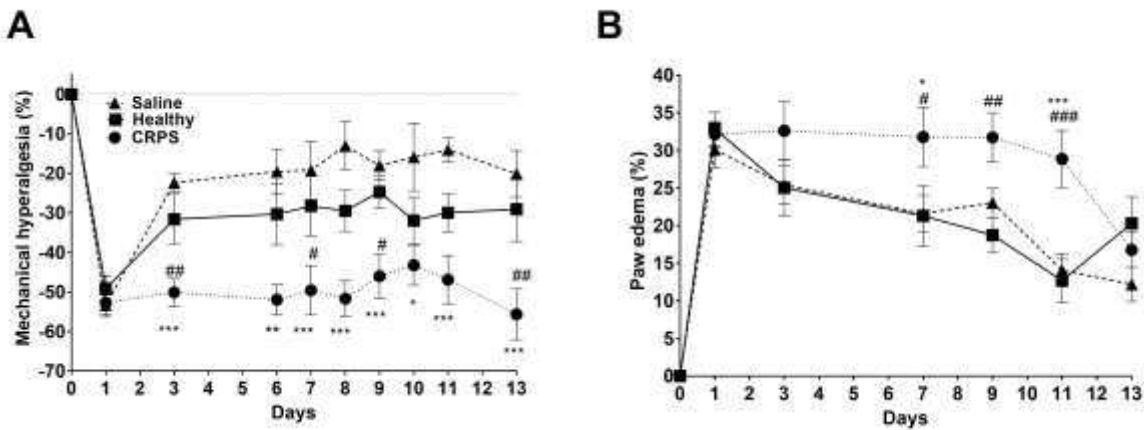
Fig. 1. Effect of intraperitoneal injection of serum IgG derived from complex regional pain syndrome (CRPS) patients or healthy controls on plantar incision-induced mechanical hyperalgesia **(A)** and swelling **(B)** of the injured mouse hindpaw. IgG was administered daily, starting on day 0. The right hindpaws were incised on day 0, about 6 h after immunoglobulin injection. Shown are pooled results from all three long-term experiments to either day 10 or day 13, with three different IgG preparations (#2, 3, 4) (see patients details in supplementary Table S1, individual results in Figure 2). Data are means $\pm$ SEM, *p < 0.05, **p < 0.01, ***p < 0.001 (vs. saline-treated control mice), #p < 0.05, ###p < 0.001 (vs. healthy IgG-treated mice); two-way ANOVA followed by Bonferroni's multiple comparison test.

Figure 2
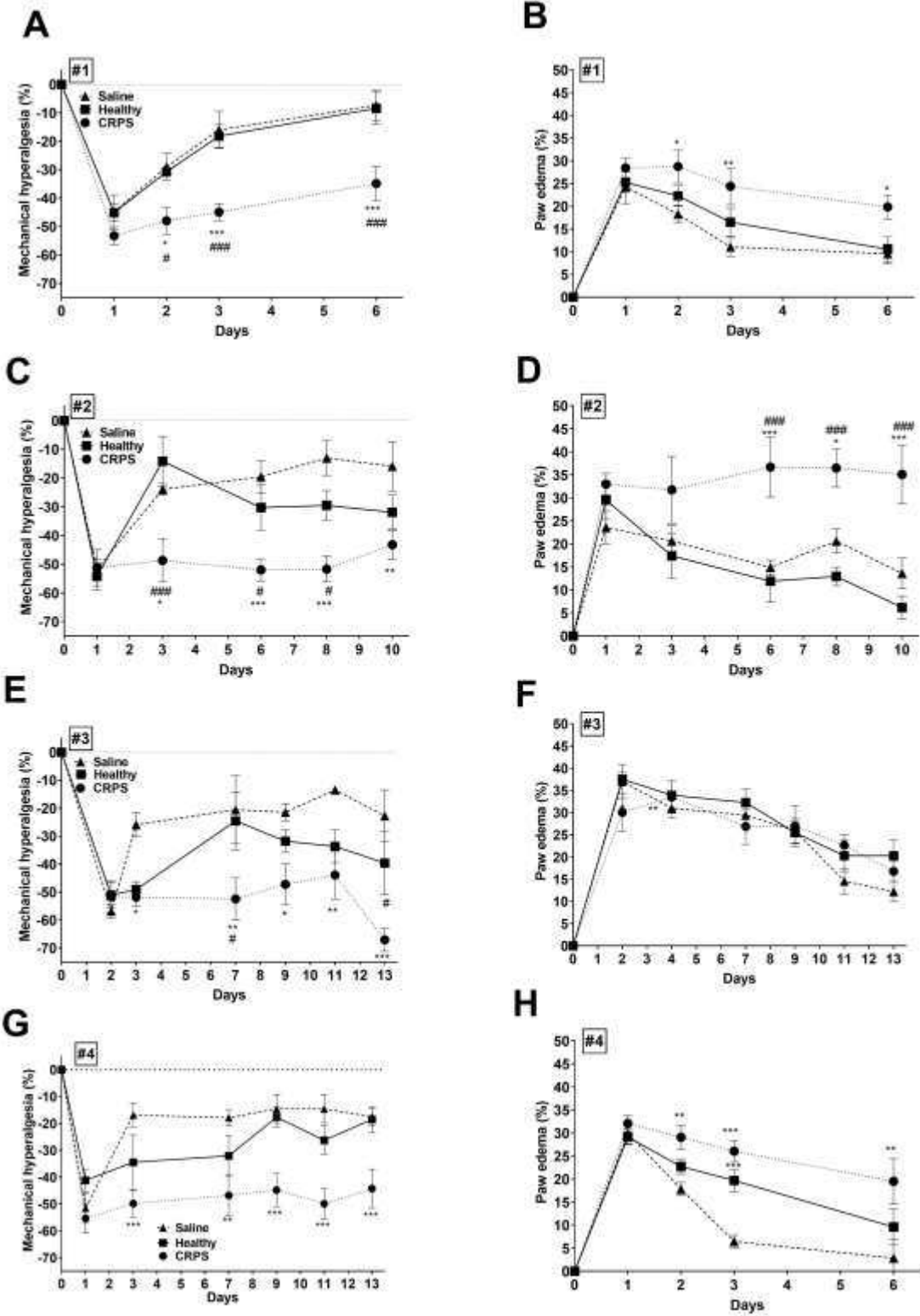
Fig. 2. Individual preparations elicit consistent, stable mechanical hyperalgesia, but variable paw swelling. Panels show behavioural data in groups of animals injected with either of four IgG preparations (patients #1,2,3,4), demonstrating patient/preparation-dependent variations and apparent lack of correlation between hyperalgesia **(A, C, E, G)** and paw edema **(B, D, F, H)**. Data are shown as means $\pm$ SEM, *p < 0.05, **p < 0.01, ***p < 0.001 (vs. saline-treated control mice), #p < 0.05, ###p < 0.001 (vs. healthy IgG-treated mice); two-way ANOVA followed by Bonferroni's multiple comparison test.

CRPS IgG does not alter vascular plasma leakage, but increases neutrophil MPO activity early after paw incision

Indocyanin green (ICG) - derived fluorescence showed a trend to increase in the injured paws in all groups two days after paw incision emphasising that CRPS-IgG did not specifically affect plasma-extravasation (saline injured: $1.52 \times 10^9 \pm 1.11 \times 10^8$; healthy IgG injured: $1.42 \times 10^9 \pm 1.54 \times 10^8$; CRPS IgG injured: $1.70 \times 10^9 \pm 2.2 \times 10^8$; fluorescence intensity: (photons/second/cm^2/steradian)/μW/cm^2).

As expected, in vivo imaging of L-012 derived bioluminescence, used as a sensitive marker of inflammatory cell activity (most prominently neutrophil-derived MPO) showed increased signal in response to limb trauma alone (Fig.3). We found significantly increased neutrophil MPO-activity in the CRPS IgG-treated animals on the affected side 2 days after the incision, when compared to the control groups. Differences in MPO-activity in CRPS IgG versus healthy IgG groups had disappeared by day 6, although significant increases in the injured paw were still present compared to the intact side on day 13. Importantly, while strong variability was seen between different IgG preparations in influencing MPO-activity (Supplementary Fig. S4 and Table S1), bioluminescence measured on day 2 or 6 did not correlate with either maximal paw swelling or hyperalgesia on day 6 (not shown). This suggests that altered MPO activity in the injured paw of tCRPS mice is an unrelated IgG effect that is unlikely to explain the marked impact of CRPS IgG on paw hypersensitivity.

Figure 3
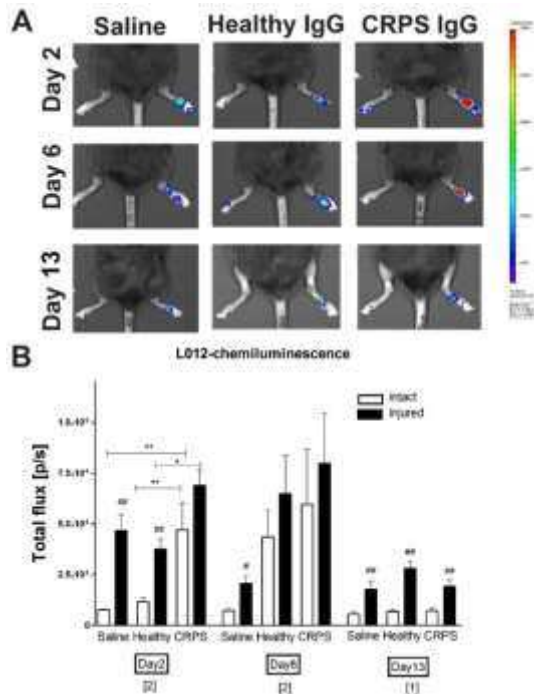
Fig. 3. Imaging reactive oxygen species demonstrates the development of inflammation in the injured hindpaws of mice. In vivo images of L-012 - derived bioluminescence were obtained during general anaesthesia on days 2, 6 and 13 after paw incision. Typical images are shown in **(A)**, and quantification of the bioluminescence-intensity in **(B)**. Data at each time point represent the pooled results from experiments conducted with separate CRPS/healthy IgG preparations (number of preparations per time point in brackets, details in the supplementary appendix Figure S4 and Table S2), and are shown as means $\pm$ SEM of n= 6-18 mice/group; *$p < 0.05$, **$p < 0.01$, ***$p < 0.001$ vs. respective control groups, #$p < 0.05$, ##$p < 0.01$ vs. respective intact side, one-way ANOVA followed by Bonferroni's multiple comparison test.

CRPS IgG does not promote inflammation or neuropathy in the paw

We further examined whether the tCRPS behavioural signs related to locally augmented inflammatory responses, or to neuropathic changes. In successive experiments, animals were sacrificed between experimental days 1-13 and paw tissues harvested to assess various inflammatory changes (animal numbers and preparations supplementary Table S3).

Substance P (SP) levels increased in the injured paw, with higher levels in the CRPS IgG group on day 6 (Fig. 4A), while calcitonin gene related peptide (CGRP) levels were not significantly altered (Fig. 4B), consistent with earlier findings (18). Increased levels of inflammatory

mediators were seen in the injured paws, with gradual decrease over time (shown in Figure 4C-F for interleukin-6 (IL-6), tumor necrosis factor α (TNF-α), monocyte chemoattractant protein-1 (MCP-1), interleukin-1 (IL-1β), and for additional mediators in the supplementary appendix S5). We detected no differences in the levels of inflammatory mediators between the CRPS and healthy IgG groups (Figure 4C-F, supplementary appendix S5) at any time point, except for a mild CRPS-IgG induced MCP-1 increase at day 13 (Fig. 4E). Notably, at the time of maximum hyperalgesia, 13 days post-injury, most mediators were undetectable. There were no significant changes in plasma concentrations of any cytokines after correction for multiple testing (supplementary appendix Fig. S6).

Histological examination revealed moderate infiltration of inflammatory cells into areas immediately adjacent to the incision early after surgery, with no obvious difference between groups, and no evidence of infiltration by inflammatory cells on day 13 in any experimental group (not shown). Since some patients with persistent CRPS exhibit mild small fibre neuropathy (23), we also examined mouse paws for any evidence of structural changes to small skin nerves with both light- and electron microscopy. The morphology of the axons in the right and left paws and the ultrastructure of non-myelinated and thinly-myelinated axons were very similar between experimental groups (Figure 5).

Figure 4
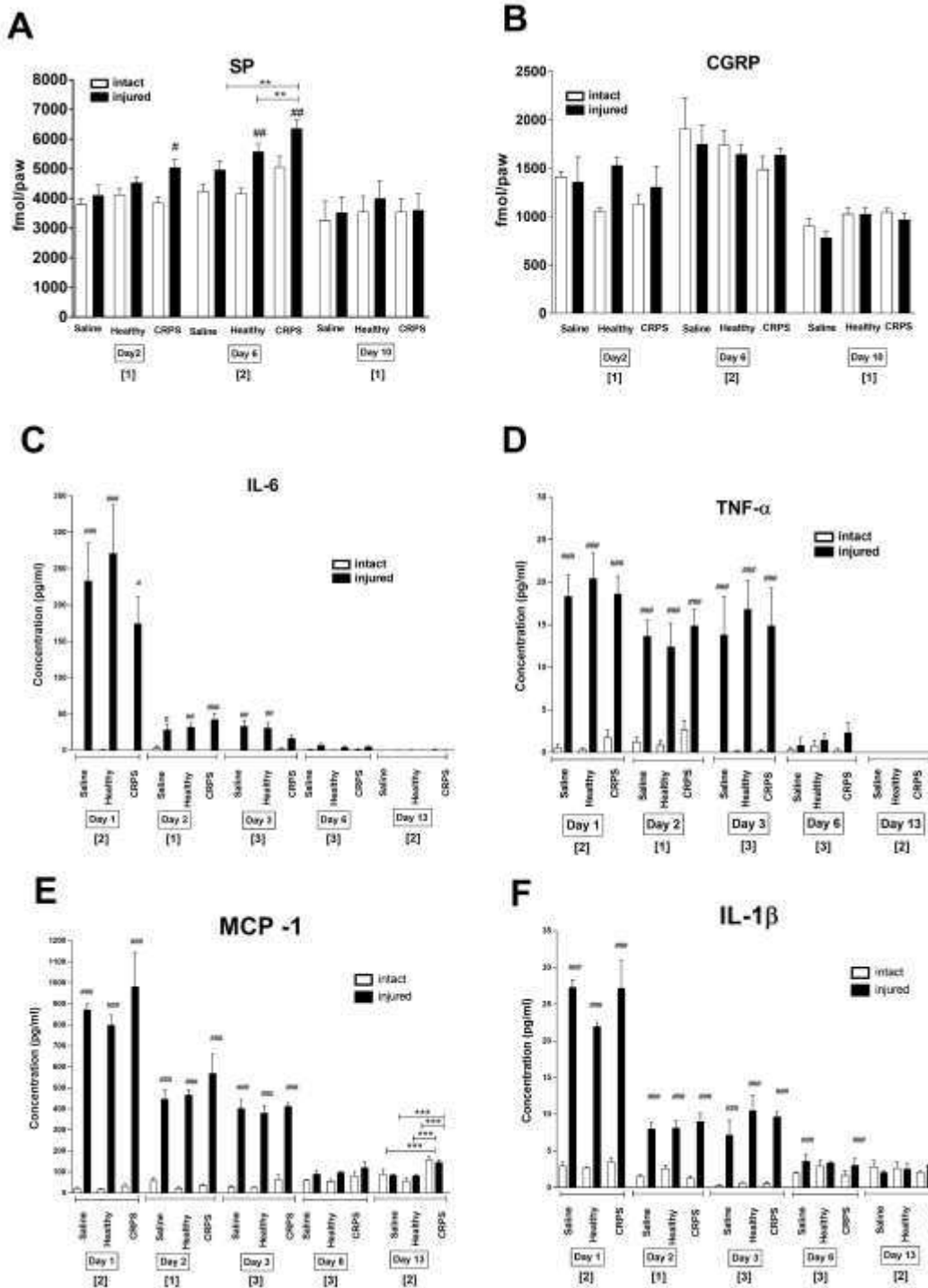
Fig. 4. Effects of human IgG treatments on sensory neuropeptide and inflammatory cytokine concentrations in the hindpaws. Concentrations of (**A**) SP and (**B**) CGRP were measured by radioimmunoassay in hindpaw homogenates excised after sacrifice. Concentrations of (**C**) IL-6, (**D**) TNF-α, (**E**) MCP-1 and (**F**) IL-1β were measured by

cytometric bead array from the same samples. Data are from 1-3 experiments per time point (bracket below x-axis) each with different patient preparations. Shown are means ± SEM; *p < 0.05, **p < 0.01, ***p < 0.001 respective control groups, #p < 0.05, ##p < 0.01, ###p < 0.001 vs. respective intact side, one-way ANOVA followed by Bonferroni's multiple comparison test.

Figure 5
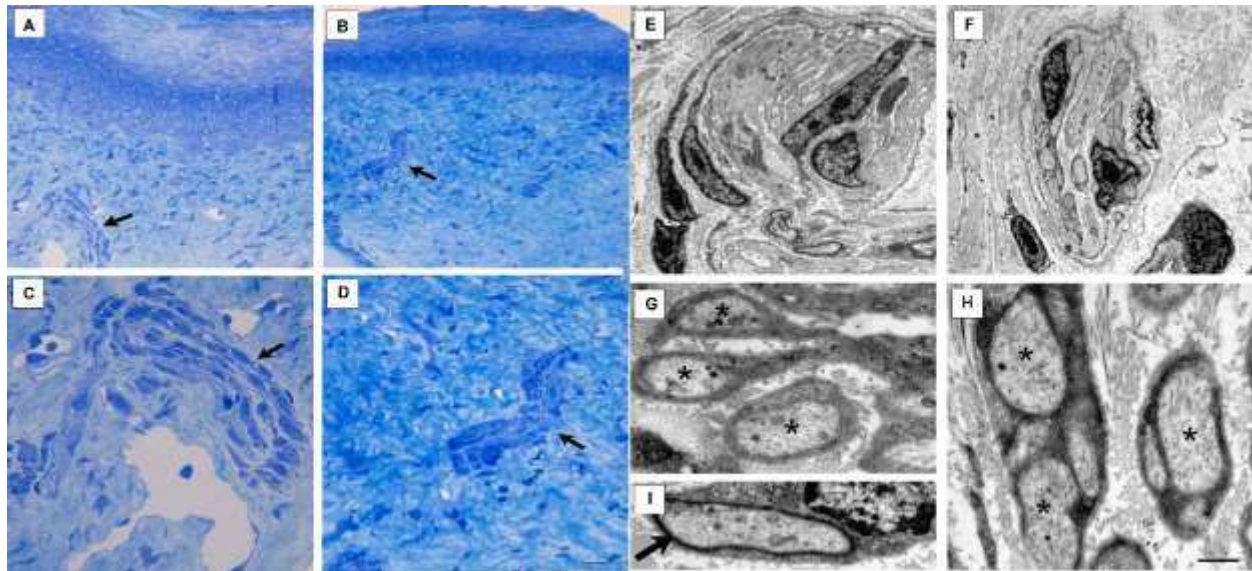
Fig. 5. Small nerve fibres in the tCRPS paw skin. **(A-D)** Semithin sections of the right **(A, C)** and left **(B, D)** paws of the CRPS group. Arrows point to bundles containing non-myelinated, thinly-myelinated and myelinated axons. Structures shown in **(A, B)** are visible in **(C, D)** with higher magnification. Scale bar is 50 µm in **(A, B)**, 20 µm in **(C, D)**. **(E-I)** Photomicrographs of ultrathin transmission EM sections of the right **(E, G, I)** and the left **(F, H)** paws of the CRPS group. **(E, F)** show small magnification images of thin nerves containing non-myelinated, thinly-myelinated and myelinated axons. **(G)** Ultrastructure of non-myelinated axons (asterisks), and **(I)** of a thinly-myelinated axon in an oblique section (arrow). **(H)** Ultrastructure of non-myelinated axons (asterisks) from the left paw. Scale bar is 3 µm in **(E, F)**, 500 nm in **(G, H)** and 750 nm in **(I)**.

CRPS-IgG facilitates sustained microglia activation in the CNS

We next investigated, whether altered activity of microglia or astrocytes in pain-related circuits (24) would reflect the marked effects of CRPS IgG on pain sensitivity responses. Glial cell counts showed a trend to increase in the ipsilateral dorsal horn and the contralateral S1 cortex at

all time points when compared to the respective mirror sides, which did not always reach significance (Fig. 6 and Fig. S7).

In CNS areas receiving input from the injured paw, CRPS-IgG induced remarkable increases in both astrocyte and microglia cell numbers when compared to both saline and healthy IgG groups. In the dorsal horn, this response was sometimes much stronger than the increases representing the incision trauma (Fig. 6). Astrocyte reactivity in the CRPS IgG animals was augmented in all CNS areas at early time points (day 3 and day 6), whereas microglia staining was enhanced throughout the experimental period including day 13 (Fig. 6 and Fig. S7). This highlights that increased mechanical hypersensitivity in this CRPS model is associated with transient astrocyte-, and persistent microglial activation in the CNS.

Figure 6
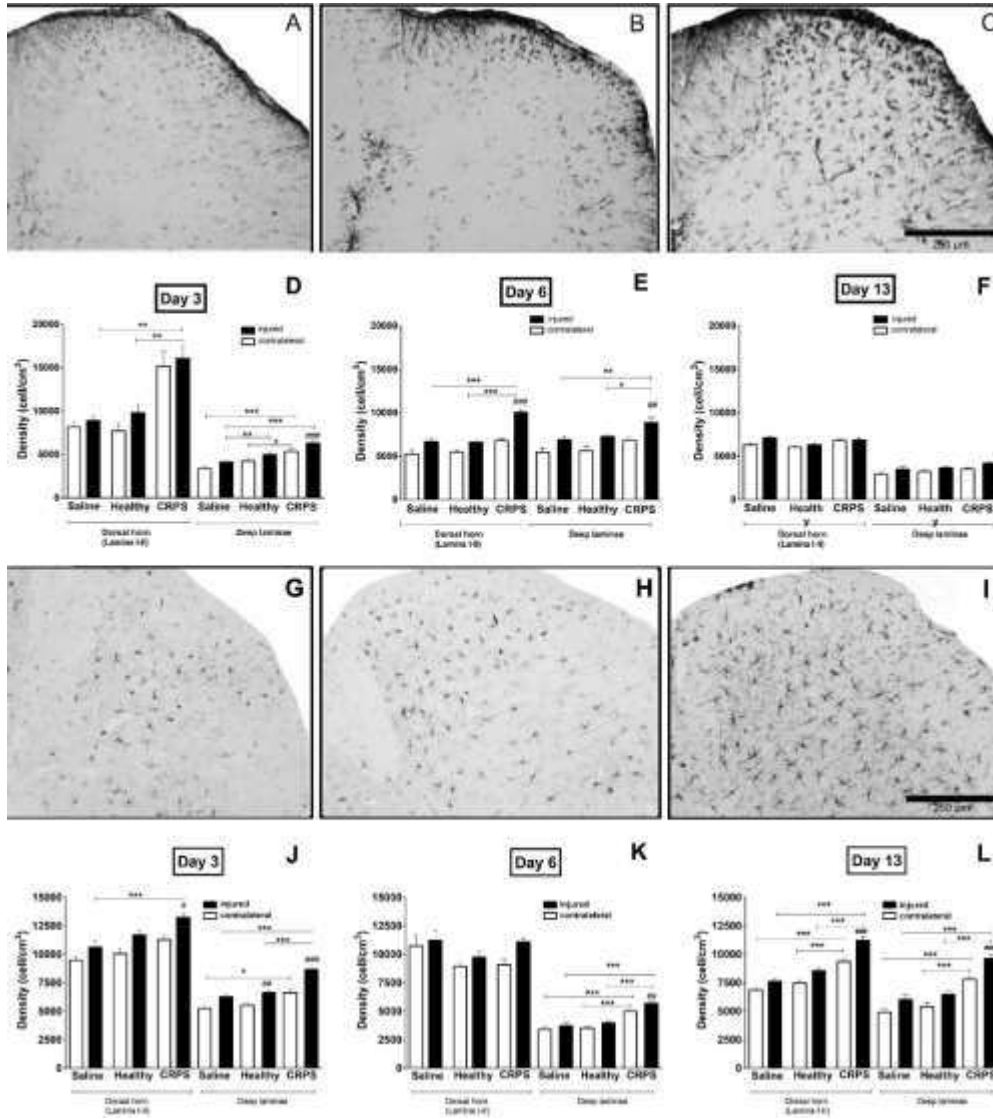
Fig. 6. Glial activation in the L5 spinal cord dorsal horn, ipsilateral to the paw injury. Panels (**A-C**) show GFAP immunopositivity marking astrocytes, and panels (**G-I**) show Iba1 immunopositivity marking microglia cells, with (**A, G**) saline, (**B, H**) healthy, and (**C, I**) CRPS. The GFAP immunopositive sections shown are from day 6-, and Iba1 sections from day 13 after paw incision. Quantification of astrocyte reactivity (**D-F**) and microglia staining (**J-L**) in lamina I-II dorsal horn of the L4-L6 spinal cord, and deeper laminae, at 3, 6, and 13 days post hindpaw incision. Each panel represents the pooled results from 2 experiments with 2 different samples (#3, #4). Shown are means ± SEM of 6-7 mice per group *$p < 0.05$, **$p < 0.01$, ***$p < 0.001$ vs. respective control groups; #$p < 0.05$, ##$p < 0.01$, ###$p < 0.001$ vs. respective contralateral side; one-way ANOVA followed by Bonferroni's modified post hoc test.

Early IL-1 receptor blockade with anakinra prevents the development of tCRPS, while delayed anakinra treatment abrogates established tCRPS and reduces glial activation.

Since both microglia and astrocytes are important sources of proinflammatory cytokines that are known to contribute to pain hypersensitivity responses (25, 26) and as interleukin-1 is a key mediator that influences neuronal activity (27, 28), we investigated the effects of steroid treatment, or interleukin-1 receptor antagonist treatment (anakinra) on CRPS-IgG induced behavioural signs and inflammatory changes. Prednisolone (4 mg/kg), or anakinra (10 mg/kg) were daily administered intraperitoneally, starting 5h prior to surgery (day 0) and extending throughout the experimental period. One day after surgery, mechanical hyperalgesia developed equally in all groups (Fig. 7. A-B). Steroid treatment transiently reduced CRPS-IgG induced mechanical hyperalgesia (between days 2 and 3), but behaviour had reverted to the abnormal course by day 7. In contrast, anakinra prevented all CRPS-IgG-induced effects throughout the experimental period (Fig.7B). Anakinra, but not steroid treatment almost completely reversed glia cell activation in the ipsilateral dorsal horn, on day 6 (Figure 7. D-E); notably anakinra treatment also significantly reduced paw MCP1 levels on day 3, but there were no other differential effects on peripheral mediator production between these two treatments (appendix Fig. S7). Delayed administration of anakinra from day 8 onwards abrogated the established tCRPS phenotype (Figure 7C), and completely reversed the associated increased dorsal horn microglia activation on day 13 (7F).

Figure 7
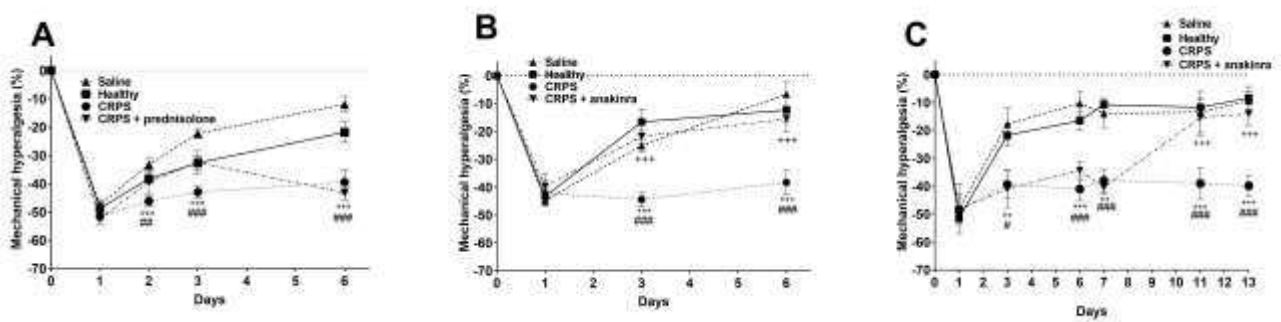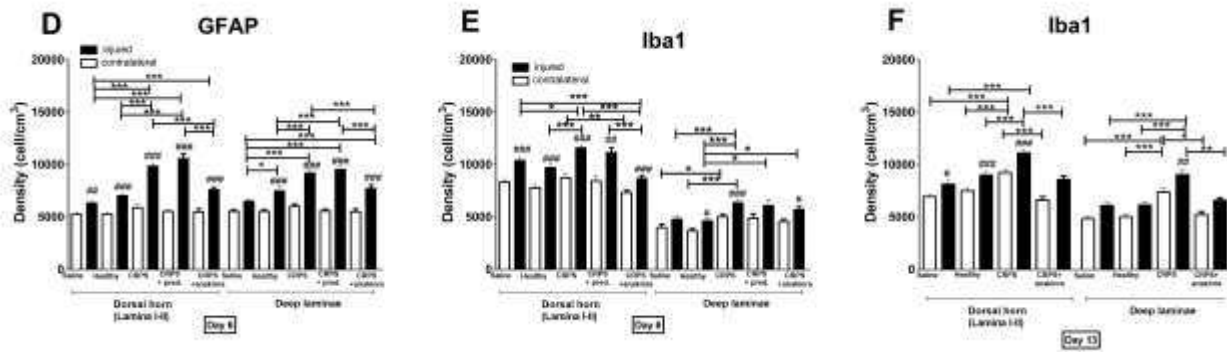
Fig. 7. Effects of prophylactic steroid or anakinra treatment (days 0-6), and delayed (therapeutic) anakinra treatment on CRPS-IgG induced mechanical hyperalgesia, and glial activation in the spinal cord. Panels **(A, B)** show mechanical hyperalgesia in groups of animals injected intraperitoneally first with human IgG or saline, and 3 hours later with 4 mg of prednisolone or 10 mg/kg anakinra, or saline vehicle, on each day between days 0-6. Panels **(D, E)** show dorsal horn glia cell activation in these mice on day 6, **(D)**: GFAP (astrocyte); **(E)**: Iba-1 (microglia). Results represent the average values derived from two independent experiments with different preparations for each treatment, four experiments in total; saline, healthy, and CRPS outcomes are pooled from these experiments. **(C, F)** - late anakinra treatment starting day 8, C - behavioural outcome, **(F)** - dorsal horn microglia cell count on day 13. Data are shown as means $\pm$ SEM. Significance symbols for the behavioural data: *p < 0.05, **p < 0.01, ***p < 0.001 (CRPS vs. saline-treated control mice), #p < 0.05, ###p < 0.001 (CRPS vs. healthy IgG-treated mice), +++p < 0.001 (anakinra + CRPS vs. CRPS IgG-injected mice), two-way ANOVA followed by Bonferroni's multiple comparison test.

Significance immunohistochemistry data: *p< 0.05, **p< 0.01, ***p< 0.001 vs. respective control groups; #p< 0.05, ##p< 0.01, ###p< 0.001 vs. respective contralateral side; one-way ANOVA followed by Bonferroni's modified post hoc test.

Selective deletion of microglial IL-1β ameliorates, while ubiquitous deletion of IL-1αβ completely prevents tCRPS.

As these results indicated that blockage of IL-1 reverses the tCRPS phenotype, and since CRPS IgG did not appear to enhance paw IL-1 but caused significant dorsal horn glia cell activation, we investigated whether tCRPS was associated with enhanced dorsal horn glia cell IL-1 production as a potential target in the observed effects of anakinra treatment. We detected IL-1β in L4/L5 dorsal horn microglia cells only in the tCRPS group (Figure 8A), while IL-1α was not detected (not shown). We then examined, whether the tCRPS phenotype would be altered by genetic knockout of IL-1. We found that CRPS IgG injected IL-1αβ KO mice developed no enhanced hyperalgesia, and showed even less post-traumatic paw swelling (Figure 9 B-C) than

mice treated with healthy IgG. To investigate whether increased microglial IL-1β production is sufficient to mediate the effects of CRPS IgG on increased mechanical hyperalgesia, we generated a novel IL-1β$^{fl/fl}$ mouse line. Exon 4-5 of the IL-1β gene was flanked with loxP sites, resulting in the generation of IL-1β$^{fl/fl}$ allele (Supplementary Fig. S9). IL-1β$^{fl/fl}$ mice were crossed with Cx3cr1^{CreER} mice (29) resulting in microglial deletion of IL-1β upon tamoxifen administration (M-IL-1β KO), while most peripheral Cx3cr1-positive cells recovered IL-1β production due to their higher turnover as shown by using other cre-dependent reporter lines previously (29). In fact, IL-1β protein levels were markedly reduced in IL-1β KO microglia after repeated intraperitoneal injections of bacterial LPS compared to WT microglia, but no changes were seen in splenic macrophages derived from tamoxifen-treated Cx3cr1^{CreER} x IL-1β$^{fl/fl}$ mice compared to controls (Supplementary Fig. S10). Elimination of microglial IL-1β significantly reduced mechanical hyperalgesia and paw edema in mice treated with CRPS IgG, although this effect was smaller than in the case of IL-1αβ KO mice (Fig. 8B-C). Total numbers of microglia were reduced in IL-1αβ KO mice but were not altered in response to microglial IL-1β deletion in the CRPS group (Fig.9D), suggesting that while microglial IL-1β is an important driver of chronic neuro-inflammation contributing to persistent pain, other IL-1β-producing cells or actions mediated by IL-1α could also contribute to CRPS symptoms in mice.

Figure 8
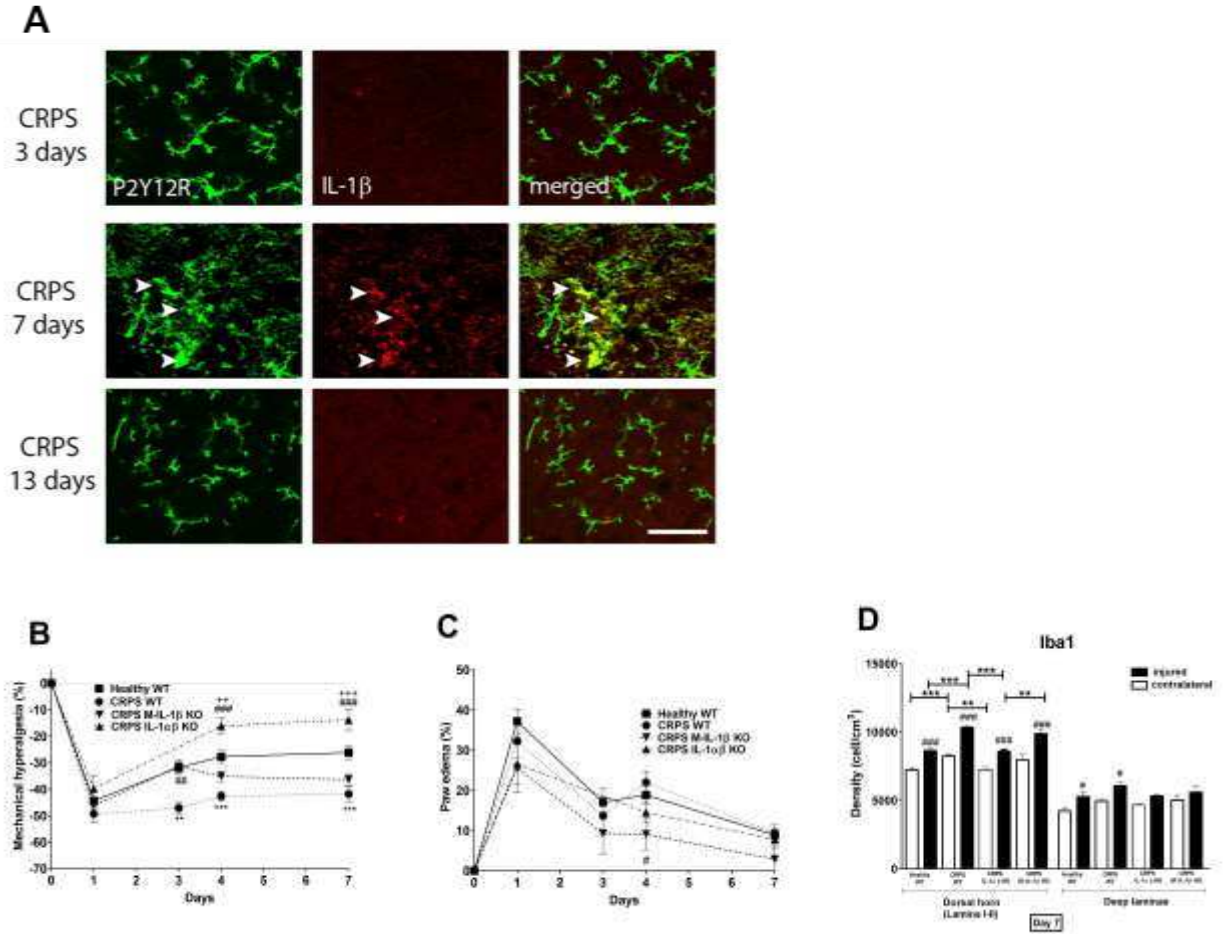
Fig. 8. Deletion of IL-*1αβ or microgl*ia-derived IL-*1β* fully or partially prevents development of the tCRPS phenotype in mice. **(A)**: A population of microglia display a morphologically activated phenotype and show immunopositivity for IL-1β at day 7 in deep laminae of the L4-L5 spinal cord near the central canal; scale bar: 50μm. **(B, C)** IL-1αβ KO mice are fully-, and M-IL-1βKO are partially protected from the development of tCRPS; **(B)** paw hyperalgesia, **(C)** paw edema. **(D)** CRPS IgG induced microglia activation is abrogated in IL-1αβ KO, but not M-IL-1β KO mice (30).

Data are pooled from two experiments with different CRPS IgG preparations for each mouse type and are shown as means $\pm$ SEM. Significance in **(B, C)**: *p < 0.05, **p < 0.01, ***p < 0.001 (CRPS WT vs. healthy WT), #p < 0.05, ###p < 0.001 (CRPS M-IL-1β KO/ CRPS IL-1αβ KO vs CRPS WT), +p < 0.05, ++p < 0.01, +++p < 0.001 (CRPS IL-1αβ KO vs. CRPS M-IL-1β KO), two-way ANOVA followed by Bonferroni's multiple comparison test. Significance values in **(D)**: *p< 0.05, **p< 0.01, ***p< 0.001 vs. respective control groups; #p< 0.05, ##p< 0.01, ###p< 0.001 vs. respective contralateral side; one-way ANOVA followed by Bonferroni's modified post hoc test.

DISCUSSION:

Here, we show in a novel, enhanced passive-transfer model that daily passive transfer of IgG from patients with persistent CRPS to mice elicits intense, unilateral static mechanical hyperalgesia after hindpaw-injury, which remains stable through the experimental period. This is associated with increased paw edema that resolves over time. Collectively, these features resemble the course and pathophysiology of the clinical disease (1). In these extensive studies, a uniform pattern of transferred static mechanical hyperalgesia was seen in all patient preparations tested, highlighting that sero-negativity is unlikely to be common in patients with severe, persistent CRPS (31).

This highlights the translational validity of the model and the importance of autoimmune mechanisms underlying the pathophysiology of both experimental and clinical CRPS. The stability and reproducibility of the transferred disease phenotype indicates the translational potential for this model to investigate the downstream mechanisms underpinning this type of chronic pain and to explore the efficacy of novel therapies.

We found that the normal, post-traumatic inflammatory response in the incised paws rapidly declined, and fully settled by day 6-13 post incision, whereas the CRPS IgG-induced increase in paw hyperalgesia remained stable throughout the experimental period, with no correlation between these two parameters. Thus, unlike in the skin of some patients with clinical CRPS (21) where this does not correlate with the clinical signs (36), we found little evidence for any CRPS IgG related enhanced paw inflammation. Our results thus demonstrate that static mechanical hyperalgesia may not depend on persistent inflammatory mediator release, indicating that transferred CRPS (tCRPS) is not a model of enhanced post-traumatic inflammatory pain. There was however some evidence for abnormal production of two specific mediators in the CRPS group: substance P production was increased at early time points, in line with some clinical observations (13, 37) and with our earlier results (18), and there was also a mild, but significant bilateral increase in MCP-1 at day 13, the role of which will require further investigations. Our findings, that treatment with anakinra from day 8 fully resolved the tCRPS phenotype, and that the absence of microglial IL-1β did not fully protect from tCRPS suggest that persistent inflammatory reaction in other cells than microglia could at least partially sustain tCRPS.

In mice, the development of tCRPS remained restricted to the injured paw, consistent with the clinical situation, where about 90% of the cases show symptoms in only one, traumatised limb (23,25). The precise mechanisms through which circulating pathogenic IgG antibodies could mediate the regional post-traumatic CRPS are presently unclear. Early, transient trauma-induced inflammatory changes or regional opening of blood nerve and blood brain barriers may play a role by promoting the expression of neo-antigens, and providing IgG access to privileged sites (1). The presence of such facilitating mechanisms is supported by our in vivo imaging results which showed plasma leakage and increased myeloperoxidase (MPO) activity in the injured paw.

MPO activity was variably enhanced in the CRPS group, without correlation with the extent of mechanical hyperalgesia or swelling. These findings may resemble the strong heterogeneity seen in patients, where the degree of limb swelling, colour changes, or temperature changes can markedly differ and these parameters don't necessarily correlate with perceived pain intensities, or recorded skin sensitivities (1).

Since inflammatory changes in the paw did not appear to explain the increased mechanical hyperalgesia in the tCRPS mice, we investigated the potential role of glial responses in pain related neuronal circuits, which have been suggested to contribute to chronification processes in post-traumatic pain models (24, 39, 40). We found that tCRPS was associated with strong microglia and astrocyte activation at all three tested levels of the nociceptive pathway, the spinal cord dorsal horn, the periaqueductal grey and the contralateral somatosensory cortex. In the dorsal horn, the extent of enhancements in the CRPS- vs control groups were sometimes several-fold higher than the extend of glia activation caused by the paw incision (Fig. 6), suggesting a powerful central effect of the transferred IgG.

We hypothesized that perioperative anti-inflammatory interventions might block regional facilitatory perioperative factors required to render circulating CRPS autoantibodies pathogenic (3). To investigate whether such interventions could reverse the disease phenotype, we treated mice peri-traumatically with high-dose prednisolone. Prednisolone temporarily interrupted the process of autoantibody-dependent sensitisation, but did not abrogate it. Systemic steroids are

considered potentially effective in very early CRPS, based on the results of one preliminary trial (41). The present data suggest that where patients produce harmful autoantibodies, the peri-traumatic application of steroids is unlikely to stop disease progression. In contrast, perioperative treatment with the IL-1 receptor antagonist anakinra consistently abrogated tCRPS-associated mechanical hyperalgesia. Notably, our results also indicated that there were only minor differences in the regional paw mediator environment after treatment with (ineffective) steroids and (effective) anakinra (Supplementary Fig. S8). Furthermore, even delayed blockade of IL-1 actions with anakinra starting day 8 after the incision-trauma when trauma-induced peripheral inflammatory responses had largely resolved, was highly effective, calling into question our original hypothesis.

IL-1 is a potent activator for astrocytes through actions via IL-1R1, whereas both activated microglia and astrocytes can contribute to painful central sensitisation though secreting IL-1 (42, 43); these actions can be effectively blocked by anakinra (44–47). In our model, augmented dorsal horn glia cell activation in the tCRPS group was fully reversed by anakinra. Since IL-1-mediated actions are involved in the cross-talk between neurons, microglia and astrocytes in promoting neuroinflammation (48, 49), we assessed glial IL-1β and IL-1α production in the spinal cord and found that microglial IL-1β production was increased on day 7 in the CRPS IgG treated group. In keeping with these data, we found that IL-1αβ KO mice were fully protected from developing the tCRPS phenotype, and associated glia cell activations. To assess the functional role of microglial IL-1β in CRPS-related hyperalgesia and swelling, we generated a novel mouse strain (IL-1β$^{fl/fl}$ mice) enabling the deletion of IL-1β from microglia. Consistent with earlier data showing prolonged cre-dependent transgene expression in long-lived microglia, but not in peripheral macrophage populations with short turnover (29), tamoxifen treatment of Cx3cr1^{CreER} x IL-1β$^{fl/fl}$ mice resulted in a marked reduction of microglial-, but not splenic, IL-1β production. As seen in IL-1αβ KO mice, the absence of microglial IL-1β production fully protected from tCRPS associated mechanical hyperalgesia up to day 3, but it had a markedly weaker effect thereafter. This highlights the importance of microglial IL-1β in the tCRPS disease process, but also the likely involvement of other cells and/or IL-1α (48). Thus, further research will be needed to clarify respective contributions of peripheral versus central elements to the transferred disease phenotype, and the cellular targets of effective future medications.

Molecular mechanisms underpinning autoantibody pathogenicity in the model, and in the clinical disease may include IgG Fab binding to sensory nerves or nearby non-neuronal cells, with consequential changes to cellular functions without triggering a systemic inflammatory response (32). The latter mechanism has recently been demonstrated to underpin non-inflammatory joint pain in rheumatoid arthritis (32, 33). The target epitopes of CRPS IgG that elicit the pertinent changes in the model remain unknown. Specific anti-autonomic autoantibodies are present in both early and late CRPS and may be involved in causing some tCRPS and clinical CRPS symptoms (34, 35).

Study strengths include the robust, multi-dimensional evaluation of a novel, enhanced CRPS disease transfer model with preparations from patients whose clinical presentations differed, using outcomes designed to provide translational validity. Further, the comprehensive assessment of both peripheral, and central markers of immune activation and of several anti-inflammatory treatments and gene knockout strategies, which has allowed a first informed suggestion for clinical studies with licenced drugs not previously reported in this patient group.

Limitations of this study include the upper transfer limit cut-off at 13 days, which was necessary to avoid the adverse effects of serum sickness (50). However, it may be argued that the 'chronic phase' in this disease model starts from the second week after incision, when peripheral inflammation and symptoms in the control group resolve. As often observed with IgG disease transfer in other disease models, tCRPS does not fully match the symptoms of clinical CRPS (51). For example, overt motor dysfunction was not detected. Independently, results apply only to the sub-group of patients with persistent (6) Budapest CRPS and a high pain intensity (NRS >7), however this is also the group of patients which presents the most difficult situation in clinic. We cannot exclude that some patients in this group don't have these antibodies. However, since each of the 7 tested sera returned the abnormal phenotype (Figures 2 and S2), the likelihood that we have missed the absence of such antibodies in more than half of patients of a similar population appears very low (< 1%, Methods 'patients' section); the development of serum diagnostic tests will be required to clarify the proportion of sero-negative patients.

In summary, we have devised a robust translational model of an 'idiopathic', post-traumatic chronic pain condition. The consistent pathogenicities of serum-IgG preparations indicate that amongst patients who have severe forms of this condition, autoantibody contribution is ubiquitous. Since abnormal signs were entirely confined to the injured side, we also established a general principle suggesting that pathogenic circulating autoantibodies can cause regionally-restricted disease when triggered by local trauma.

Our results support previous clinical observations that patients with persistent CRPS should respond to immune treatments with a reduction of at least some of their disease features (52). The clinical use of interleukin-1 receptor antagonists in CRPS has a broad therapeutic potential. Anakinra is safe, clinically licensed both in the US and Europe, and short-term use has an acceptable side effect profile (53, 54). Since CRPS regularly develops in the context of elective operations, such as arthroscopy or bunion surgery, prevention of such cases would have very important implications for both patients and procedure-related healthcare, as well as societal costs (55, 56). Furthermore, in patients who will develop CRPS post-fracture trauma can often be identified early on by their high pain intensity (57, 58), and thus, early post-operative drug-intervention may also be feasible (59).

The effects of blocking IL-1 actions with anakinra when treatment is initiated at later time points after trauma, and the duration of the beneficial effects after the drug is withdrawn should now be investigated in the present experimental model. In addition, identifying the exact cellular targets for IL-1 actions in the pathophysiology of CRPS could facilitate the development of alternative IL-1 targeting approaches in the prevention or treatment of the disease.

MATERIALS AND METHODS

Patients and serum preparation

Ethics permission was obtained to repeatedly sample larger volumes of additional CRPS patient sera (n=2), and healthy control sera (15/NW/0467, NorthWest Ethics Haydock, UK). Waste plasma was obtained between 2014-2017 from patients (n=5) newly undergoing plasma exchange treatment for persistent CRPS (20) at the Walton Center NHS Foundation Trust, a

tertiary care hospital in Northern England (UK). Use of waste-plasma does not require ethics committee approval; all patients provided individual written informed consent. The patients' baseline characteristics are provided in the Table 1. We calculated the probability that we missed an event rate of >50% of patients having no pain-sensitising autoantibodies by (0.5 ^ (number of experiments x fraction of positive experiments)): 0.5 ^ 7= 0.008125, i.e. <1%.

Small volumes of serum were pooled from samples taken at screening from all participants in a recent clinical trial (2) (n=7) who had baseline pain intensities of ≥ 7/10. Their demographics and baseline characteristics are provided in the supplementary appendix, Table S1. The patients had provided written informed consent for the use of their serum samples for research purposes, as part of their overall consent for this study.

IgG was prepared from plasma or serum of patients as previously described, using Protein G columns for affinity purification, followed by elution, buffering, dialysis in normal saline, and concentration to about 8 mg/ml immunoglobulin G for injection (pooled preparations 12mg/ml) (18).

Table 1

Number	Sex/ age	Limb/DD	Pain	Budapest	Type	Plex
#1	M/ 62	U/ 9	10	+	II	Y
#2	F/ 37	L/ 15	7.5	+	I	N
#3	F/ 38	L/ 10	9.5	+	I	Y
#4	F/ 36	L/ 10	7	+	I	Y
#5	F/ 40	L/ 5	7.5	+	I	Y
#6	F/ 51	L/ 8	8	+	I	N
#7	F/49	L/7	8	+	I	Y

Table 1. Baseline characteristics of the patient serum donors. Age= age in years at the time of plasma/serum acquisition; Limb=affected limb, DD=disease duration in years, Pain=24h average pain intensity on a 11-point numeric rating scale (0-10, with 10=pain as bad as you can imagine), Budapest=Budapest research diagnostic criteria (new IASP criteria); Type= CRPS type, where II denotes with/I=without trigger injury to a major nerve, Plex=plasma derived from plasma exchange

Animals

Since CRPS affects women 2-3 times more frequent than men, experiments were carried out on female C57Bl/6 mice (10-12 weeks-old, 18-22 g). The original breeding pairs were purchased from Jackson Laboratories (USA) through Charles River Hungary. The animals were bred and

kept in the conventional animal house of the Department of Pharmacology and Pharmacotherapy of the Medical School, University of Pécs at 24 °C, in a 12 h light–dark cycle and provided with standard rodent chow and water ad libitum. Mice were housed in groups of 5–10 in polycarbonate cages (330 cm^2 floor space, 12 cm height) upon a bedding consisting of wood shavings.

Animal ethics statement

All procedures were performed according to the 1998/XXVIII Act of the Hungarian Parliament on Animal Protection and Consideration Decree of Scientific Procedures of Animal Experiments (243/1988), complied with the recommendations of the International Association for the Study of Pain. Ethical approval was given by the Ethics Committee on Animal Research of University of Pécs according to the Ethical Codex of Animal Experiments (licence No.: BA02/2000-31/2016).

Experimental design

After acclimatization and conditioning, 3 control measurements of nociception and paw volume were performed on days -4, -3, and -2. 'Day 0' was the starting day of intraperitoneal injections (Figure S8). Mice (5–7 per group) were treated daily with 1 ml of IgG fractions (8 mg/ml) obtained from CRPS patients or healthy volunteers, or saline.

About 6 h after the injection on day 0, a standardized incision trauma was applied to the right hind-paw (see below). All mice removed their stitches within 16 hours post-surgery.

Measurements (see below) were performed repeatedly, starting on day 1, until the respective termination day.

Animals were sacrificed at various time-points (days 1, 2, 3, 6, 10, 13 post trauma), and tissue was harvested to analyse immunological alterations in the paw, and neurochemical changes in the central nervous system. Mice were deeply anesthetized with sodium-pentobarbital (100 mg/kg i.p.) their hindpaws were harvested, frozen in liquid nitrogen, and kept at -80 °C for later analysis of tissue neuropeptides and cytokine production levels. Animals were then immediately perfused transcardially with PBS followed by 4% paraformaldehyde, and the whole brains and spinal cords were excised and prepared for further immunohistochemistry analyses.

Plantar skin and muscle incision

To model a CRPS-triggering injury, we used the hindpaw plantar skin- muscle incision method under general anaesthesia as described earlier (18, 60). This model evokes a significant decline of the mechanonociceptive threshold, with a maximum 1 day after surgery, which persists for 7–8 days. Briefly, mice were anesthetized with ketamine (100 mg/kg; Calypsol, Gedeon Richter Plc., Budapest, Hungary) and xylazine (10 mg/kg; Sedaxylan, Eurovet Animal Health B.V., Bladel, Netherlands) on day 0. The operation site was prepared in a sterile manner, and the plantar surface of one right hindpaw was incised longitudinally, starting 0.2 cm from the heel, over a distance of 0.5 cm, intersecting the skin, fascia and plantar muscle. The skin was then opposed with interrupted stitches, using 5-0 nylon. The wound site was treated with povidone iodine solution.

All measurements were carried out by two investigators (VT and NS), who were blinded to treatment-assignment. Blinding was performed by the technician who performed all injections but who was otherwise not involved in the study. 'She differentially coded the animal cages and provided the decoding-key after completion of the last measurements.'

Determination of the mechanosensitivity of the paw

Most patients with CRPS, have, in addition to their spontaneous pain, also pain with the application of pressure to the CRPS-affected limb ('mechanical hyperalgesia') (31), and all patients included into this study experienced this feature. The corresponding mechano-nociceptive threshold of the plantar surface of the mouse hindpaw was determined with a dynamic plantar aesthesiometer (Ugo Basile 37400, Comerio, Italy) - a modified electronic von Frey technique-, as previously described (18, 61). The blunt-end needle exerting an increasing force to the mouse paw provides a mild, but basically painful stimulus activating Aδ and C fibres (62). Threshold decreases are considered as mechanical hyperalgesia, and are expressed as percentage decrease of the mechano-nociceptive thresholds compared to the baseline values (63–65).

Paw volume measurement

Limb swelling is a common feature of CRPS-affected limbs, and all included patients reported intermittent limb swelling. Mouse-paw volume was measured using plethysmometry (Ugile

Basile Plethysmometer 7140, Comerio, Italy). Edema was expressed as a percentage increase compared to the baseline paw volume (65, 66).

In vivo optical imaging of plasma leakage with indocyanin green extravasation

The mechanisms underpinning CRPS IgG enhanced paw swelling are unknown, but one possibility is augmented plasma extravasation. Intravenously injected indocyanine green (ICG), a fluorescent cyanine dye, binds to plasma proteins and remains in the healthy vasculature. Under inflammatory conditions it can be used to evaluate capillary leakage. ICG (0.5 mg/ kg) was dissolved freshly in 5 w/v% aqueous solution of Kolliphor HS 15 and a macrogol-based surfactant (67), and injected intravenously (retrobulbar sinus) under ketamine – xylazine anesthesia (100 mg/kg and 10 mg/ kg, i.p., respectively) two days after the paw incision. Fluorescence imaging was performed 20 minutes post injection, using a IVIS Lumina II in vivo optical imaging system (PerkinElmer, Waltham, MA, USA; auto acquisition time, f/stop = 1, binning = 2, excitation: 745 nm, emission filter: >800 nm). Identical Region of Interests (ROIs) were applied around both hindpaws up to ankles, and calibrated units of the luminescence (total radiance (total photon flux/s)) originating from the ROIs were analysed Fluorescence was expressed as total radiant efficiency ([photons/s/cm2/sr]/[μW/cm2]) (68).

In vivo optical imaging of neutrophil myeloperoxidase (MPO) activity as a marker of cellular inflammation

A luminol analogue chemiluminescent probe, L-012 (8-amino-5-chloro-7-phenylpyrido[3, 4-d]pyridazine-1,4(2H,3H) dione; Wako Pure Chemical Industries Ltd, Japan) was used for in vivo visualisation of reactive oxygen and nitrogen species (ROS/RNS) produced by MPO in neutrophils and macrophages (69, 70); L-012 has a high sensitivity towards ROS/RNS (71, 72). On days 2, 6 or 13 following incision, mice were anaesthetised by ketamine (100 mg/kg; Calypsol, Gedeon Richter Plc., Budapest, Hungary) and xylazine (10 mg/kg; Sedaxylan, Eurovet Animal Health B.V., Bladel, Netherlands), hair was removed from both hind legs to prevent scattering/absorbing of the light signal. L-012 (25 mg/kg) in sterile phosphate-buffered saline (PBS, 20 mg/ml) was injected i.p.. Bioluminescence was measured 10 min post-injection using the IVIS Lumina II in vivo optical imaging system (PerkinElmer, Waltham, USA; 180 s aquisition, F/stop = 1, Binning = 8). Data were analysed using Living Image® software (Perkin-

Elmer, Waltham, USA). Identical Region of Interests (ROIs) were applied around both hindpaws up to ankles, and calibrated units of the luminescence (total radiance (total photon flux/s)) originating from the ROIs were analysed (73, 74).

Measurement of sensory neuropeptides, inflammatory cytokines and nerve growth factor in the paw and cytokines in the plasma

Pro-inflammatory neuropeptides, peripherally released from sensory nerves (75) and inflammatory cytokines released by peri-neuronal cells (21) are abnormal in some patients with CRPS, and we measured their concentrations in the model.

The preserved frozen paws (see above) were thawed, chopped, and then homogenized in Triton X-100 and Calbiochem Protease Inhibitor Coctail containing Tris-HCl homogenisation buffer at 0 °C. In every case, 400 µl homogenisation buffer was used for 50 mg tissue sample weight to normalise the difference of the sample size. The homogenate was centrifuged at 15,000-20000 g for 20 min at 4 °C and the supernatant was immediately removed for measuring inflammatory sensory neuropeptides and cytokines. We measured CGRP- and SP-like immunoreactivities in the paws by a sensitive radioimmunoassay techniques developed in our lab, which was previously described (18, 76, 77).

Concentrations of IL-1α, IL-1β, IL-6, TNF-α, KC (CXCL1), MCP-1, G-CSF, RANTES (CCL5), IFN-γ, IL-4 and IL-10 in mouse plasma and the paw homogenates were measured by cytometric bead array (CBA) as described (47, 78), using BD™ CBA Flex Sets (Franklin Lakes, New Jersey USA) according to the manufacturers' protocol. Samples were acquired using a BD FACSVerse flow cytometer and data analysed by FCAP Array v3 software (BD Biosciences). Concentrations of nerve growth factor (NGF) and transforming growth factor beta (TGF-β) in the paw homogenates was measured by Sandwich ELISA kit (ChemiKine™, Merck, Germany) according to the manufacturers' protocol. `The concentrations of all cytokines and chemokines were expressed as pg mediator per ml wet tissue homogenate (79).

Paw skin light and electron microscopy

Following biopsy, samples were immersed into a fixative containing 2.5% glutaraldehyde buffered with phosphate buffer (PB, 0.1M, pH 7.4) for overnight at 4°C. Blocks then were fixed in 1% osmium tetroxide for 35 min and dehydrated with increasing concentration of ethanol.

After complete dehydration in ascending ethanol series blocks were transferred to propylene oxide before being placed into aluminum-foil boats and then embedded into gelatin capsule containing Durcupan resin (Sigma, Budapest, Hungary).

Semithin and ultrathin sections were cut with Leica ultramicrotom. Semithin sections were mounted on glass slides, stained with toluidine blue and examined under light microscope. Ultrathin sections were mounted on collodion-coated (Parlodion, Electron Microscopy Sciences, Fort Washington, PA) single-slot copper grids, contrasted with uranyl-acetate and lead-citrate, and were examined in JEOL 1200EX-II electron microscope.

Immunohistochemistry detection of central nervous system glia cells

Brains and L4-L6 segments of the spinal cord were removed and post-fixed for 4 h in 4% paraformaldehyde before being placed into 30% sucrose (Duchefa Biochemie, Netherlands) in 0.1 M PBS overnight at 4°C. Spinal cord and brain sections (30 µm) were prepared using a freezing microtome (Leica Biosystems Nussloch GmbH, Germany) as free floating sections (80, 81). Sections were washed in 0.05M Tris buffered saline (TBS, pH 7.6), incubated in 0.3% H_2O_2/ methanol (Szkarabeusz Ltd, Hungary) for 30 min to inhibit endogenous peroxidase activity, followed by washing steps. Samples were incubated in primary antibodies for 48 hours at 4°C (GFAP dilution: 1:1000, Novocastra™ Leica Biosystems and Iba1; dilution: 1:500, Wako Chemicals GmbH, Germany). After washing steps, sections were incubated with Vectastain Elite ABC HRP Kit (Vector Labs, USA). The bound antibodies were visualized using Nickel (II) sulfate hexahydrate/3,3′-diaminobenzidine tetrahydrochloride (DAB, Sigma-Aldrich, USA) as chromogen, and glucose oxidase (Sigma-Aldrich, USA), which resulted in a black precipitate within the labelled cells.

The sections were mounted onto gelatinized slides, allowed to dry overnight, dehydrated through increasing concentrations of ethanol; they were then coverslipped with DPX (Sigma-Aldrich, USA), and allowed to dry again.

Three brain and spinal cord sections/mouse (n=3-4 animal/ group) were examined by Neurolucida software (v07, MBF Bioscience, USA) using Nikon Eclipse Ni-E bright field microscope with a computer controlled stage. The quantitative analysis was carried out using a modified unbiased stereology protocol as previously described (82). GFAP or Iba1

immunoreactive cells were examined in standardized areas of laminae I-II (superficial), and deep laminae of the dorsal horn of L4-L6 spinal cord sections, lateral periaqueductal grey matter, and the somatosensory hindpaw cortex (83, 84).

Cell counting was conducted as follows: we traced the contours of the specific areas under low magnification (4x) with the help of Paxinos and Franklin mouse brain atlas (85), then we counted labelled astrocytes and microglia cells using higher magnification (10x). Since the thickness of the section was 30 µm, cells were counted in a 3-dimensional tissue and we calculated the 3D cellular volume using Neurolucida software. The density of GFAP and Iba1 immunopositive cells was determined as the number of counted cells divided by the volume of the measured area, expressed as cell number/ cm^3 (86).

Assessment of the preventive effect of peri-traumatic immune suppression

We investigated whether early immune suppression would alter the disease course in the model. We administered the synthetic glucocorticoid prednisolone (4 mg/kg, i.p. (87, 88), or the IL-1 receptor antagonist anakinra (10 mg/kg, i.p, Swedish Orphan Biovitrum AB (publ), SE-112 76 Stockholm (89)). Control animals received respective vehicles. The first drug injection was 3 h prior to the plantar skin and muscle incision, and at least 4 h after IgG, or control treatment. Drug treatment was then repeated daily through the experimental period.

Immunofluorescence

25 µm thick free-floating brain sections were with 5% normal donkey serum and incubated overnight at 4C° with the appropriate mixture of primary antibodies: rabbit anti-P2Y12 (dilution 1:500, #55043A, AnaSpec), goat anti-IL-1α (dilution 1:500, #AF-400-NA R&D Systems), and goat anti-IL-1β (dilution 1:500, #AF-401-NA R&D Systems). For visualization donkey anti-rabbit Alexa 488 and donkey anti-goat Alexa 647 secondary antibodies (1:500) were used. Images were captured with a Nikon Ni-E C2+ (Nikon, Tokyo, Japan) confocal microscope, and image processing was performed using the NIKON NIS Elements Viewer 4.20 software (Auroscience Ltd., Budapest, Hungary).

Generation of IL-1 beta floxed mice

Il1b$^{tm1a(EUCOMM)Hmgu}$ embryonic stem cells (90) were purchased from the European Mouse Mutant Cell Repository (EuMMCR). Cells from clone HEPD0840-8-E03 were prepared for microinjection according to previously published protocol (91) with minor modifications. Briefly, ES cells were cultured in KO-DMEM + KOSR + 2i (MEK inhibitor and GSK3 inhibitor) on a gelatinized (0.1% gelatin in PBS) cell culture dish maintained in standard culture conditions (37°C, 5% CO_2, humidified). The culture medium was changed daily and the cells were passaged when 75-80% confluent using accutase to dissociate the cells. Cells were passaged no more than 3 times, and were transferred to media without 2i reagents for 24 hours prior to microinjection. Cells were then microinjected into 4 to 8 cell B6N-Tyr^{c-Brd}/BrdCrCrl embryos. Surviving embryos were surgically implanted into the oviduct of day 0.5 post-coitum pseudopregnant mice. Resulting black/white C57BL/6N chimeras were back-crossed onto C57BL/6N wild-type mice to assess germline penetrance. Potential founder mice were screened by PCR for LacZ, Neo and LoxP sites. This line was further crossed with C57BL/6N-Tg(CAG-Flpo)1Afst/Mmucd mice. The flp recombinase expression provided by this line resulted in a "conditional ready" (floxed) Il1b$^{tm1c(EUCOMM)Hmgu}$ allele where exons 4 and 5 are flanked by loxP sites.

Statistical analysis

Data shown are means ± SEM, and two-way repeated measures ANOVA followed by Bonferroni's post hoc test was used for comparison of threshold values between groups at respective timepoints. One-way ANOVA followed by Bonferroni's post hoc test was used for analysis of the immunochemistry and cytokine results. A value of $p < 0.05$ was considered statistically significant.
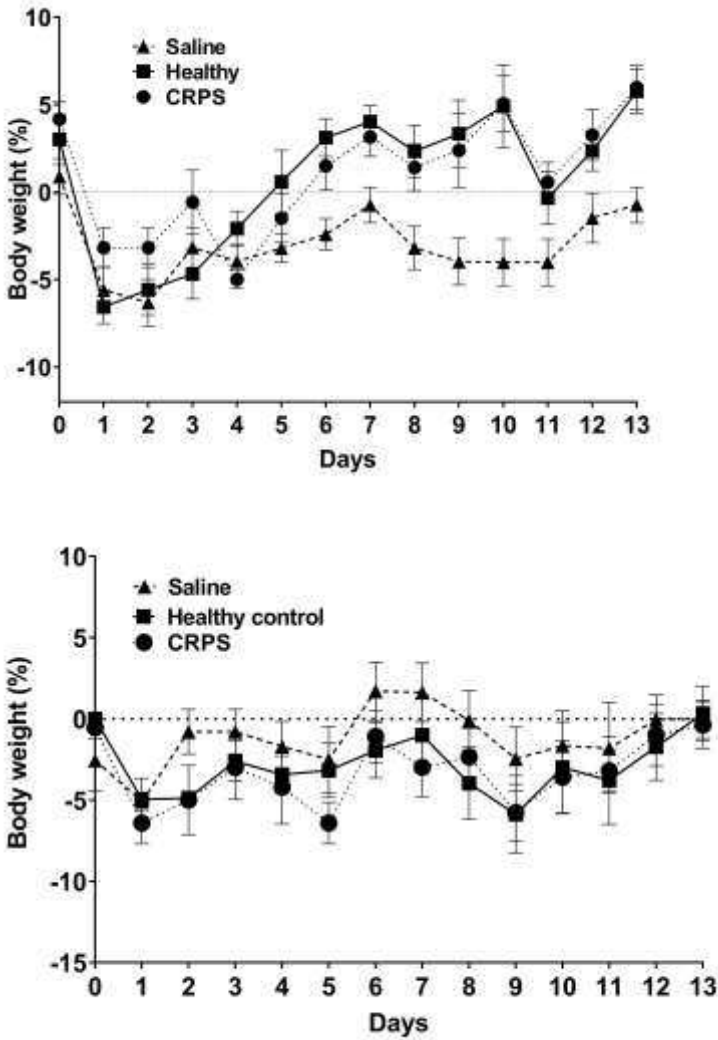
Figure S0

Figure S0. Typical weight change over time. Minimal weight loss was observed in all groups reaching a nadir at 3-4 days after surgery, followed by recovery. Values are in percent of baseline (the average of 3 measurements in the preceding week). Error bars denote SEM.

Table S1

| R-no	Baseline
P01002	6.8
P01004	*9.3
P01005	*8.2
P01006	*8.4
P01009	*7.2
P01012	5.9
P01001	*7.6
P01003	6.8
P01007	6.6
P01008	6.2
P01010	*8.5
P01011	*9.1

Table S1. Pain intensities at baseline of all randomized patients in the MYPS trial, and of seven patients selected for pooled testing in the passive-transfer model. R-no= randomization number; baseline= pain intensity at baseline (average of daily average pain intensity ratings on a 0-10 numeric rating scale, during the screening period, maximally 14 entries); *denotes patients whose serum was used for a pooled experiment, see methods section ('patients and serum preparation') and Figure S2 G-H. Adapted from (58), Table W1.

Figure S1
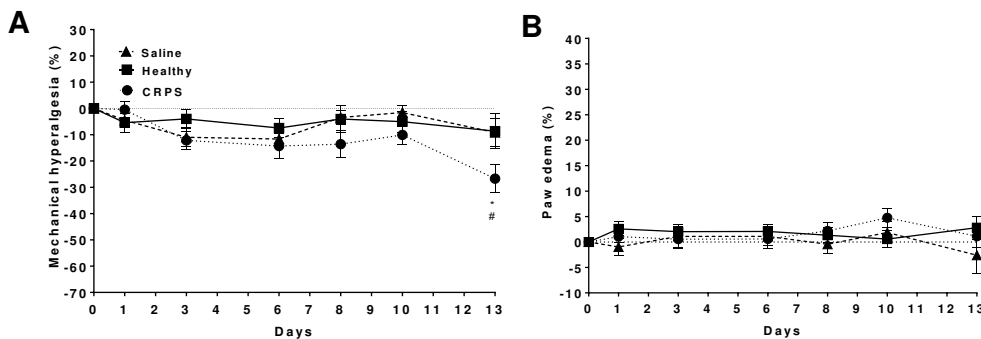
Fig. S1. Effect of serum IgG derived from complex regional pain syndrome (CRPS) patients or healthy controls, or saline on mechanical hyperalgesia (**A**) and swelling (**B**) of the intact hindpaw. Pooled results from the three long-term experiments up to day 13 (injured-paw results: Figure 2). Data are means $\pm$ SEM, *p < 0.05 (vs. saline-treated control mice), #p < 0.05 (vs. healthy IgG-treated mice); two-way ANOVA followed by Bonferroni's multiple comparison test.

Figure S2
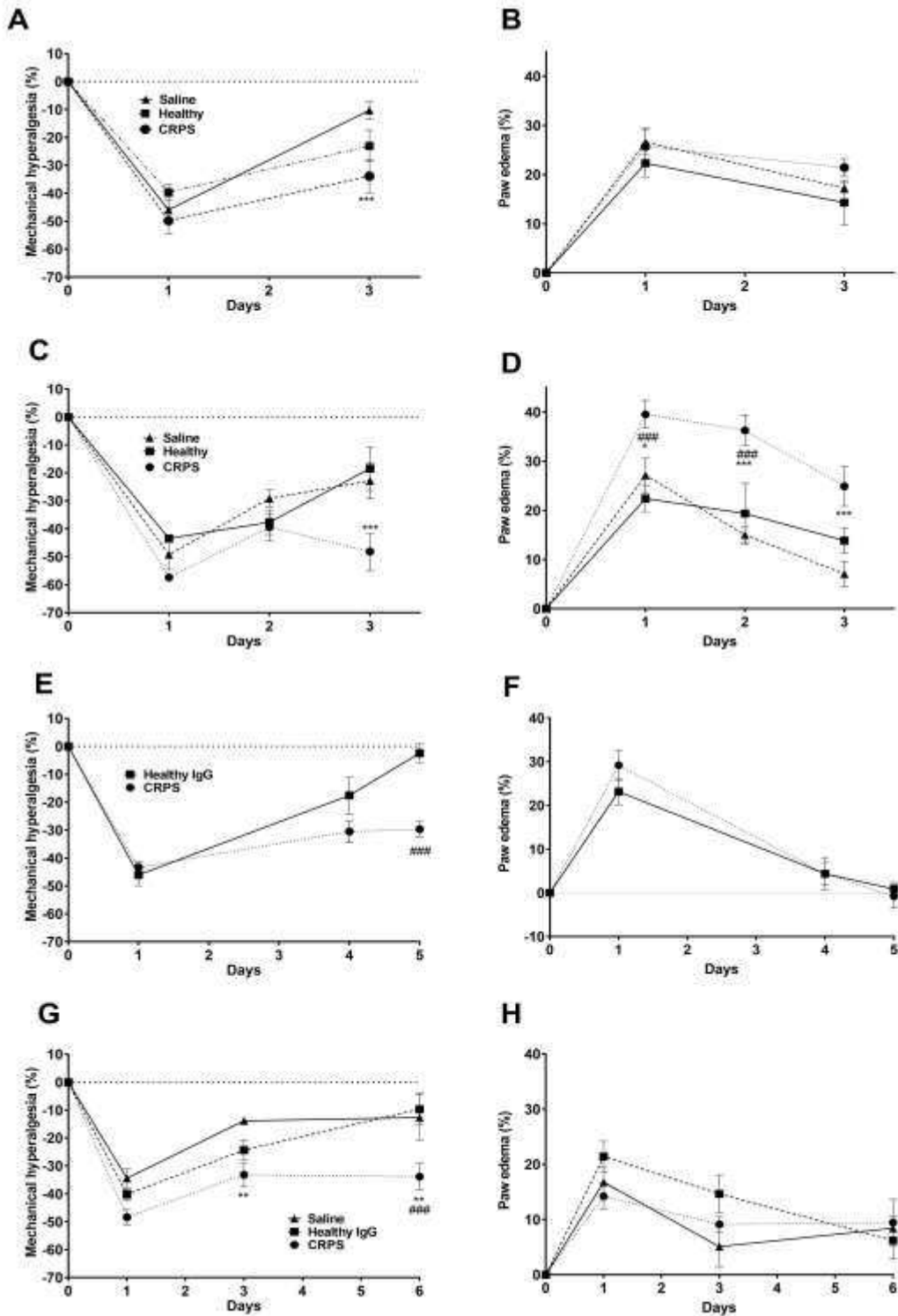
Fig. S2. Behavioural effects of injection with CRPS/healthy serum-IgG samples not used in long behavioural experiments, and pooled samples from the MYPS trial. (**A-F**): effect of serum-IgG derived from complex regional

35

pain syndrome patients #5-#7 (Table 1), or healthy controls, or saline on plantar incision-induced mechanical hyperalgesia and swelling; G-H: results from the injection of sera pooled from 7 patients (Table S1) with data are shown as means $\pm$ SEM, *p < 0.05, ***p < 0.001 (vs. saline-treated control mice), ###p < 0.001 (vs. healthy IgG-treated mice); two-way ANOVA followed by Bonferroni's multiple comparison test.

Figure S3
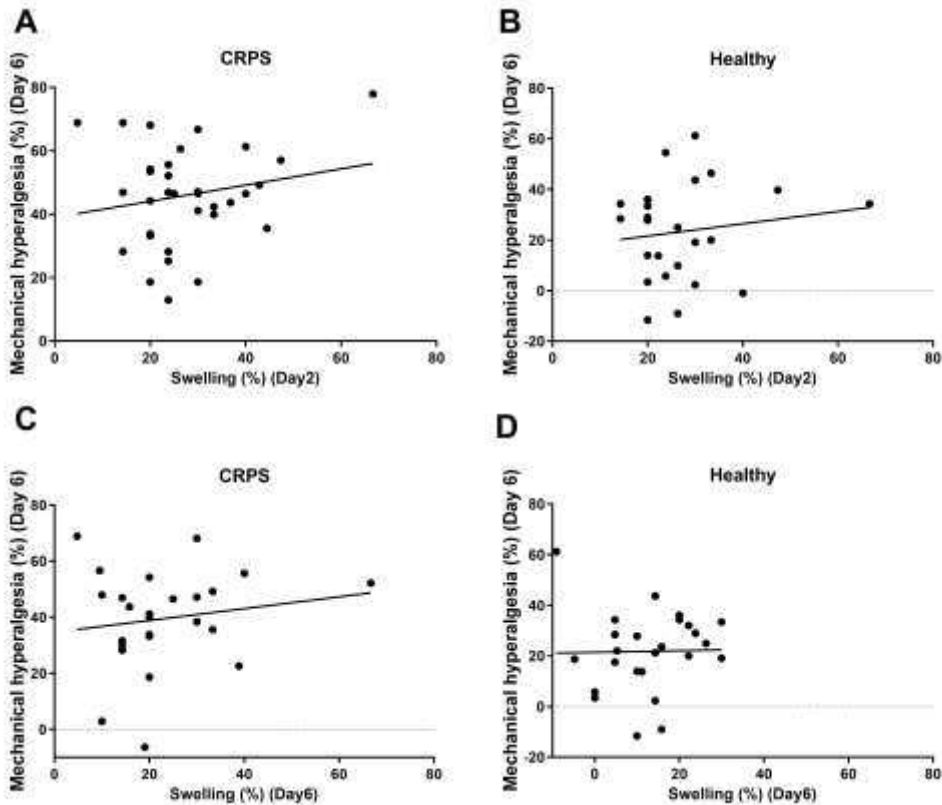
Fig. S3 Correlation between mechanical hyperalgesia and paw swelling. Panels **(A, B)** show correlation between the mechanical hyperalgesia on day 6 and to paw edema on day 2 (when this was usually maximal), while **(C, D)** show correlations between both parameters on days 6 respectively. Dot plot data represent individual animal data, as obtained from 4-5 experiments using different patient preparations per time point, 6 mice/ experiment. There is no correlation at any measured time point. **(A, B)** n=30-32 animals; Spearman r=0.056; p= 0.741 in CRPS group and r=0.103; p=0.632 in healthy group. **(C, D)** n=24-26 animals; Spearman r=0.116; p=0.577 in CRPS group and r=0.202, p=0.331 in healthy group.

Figure S4
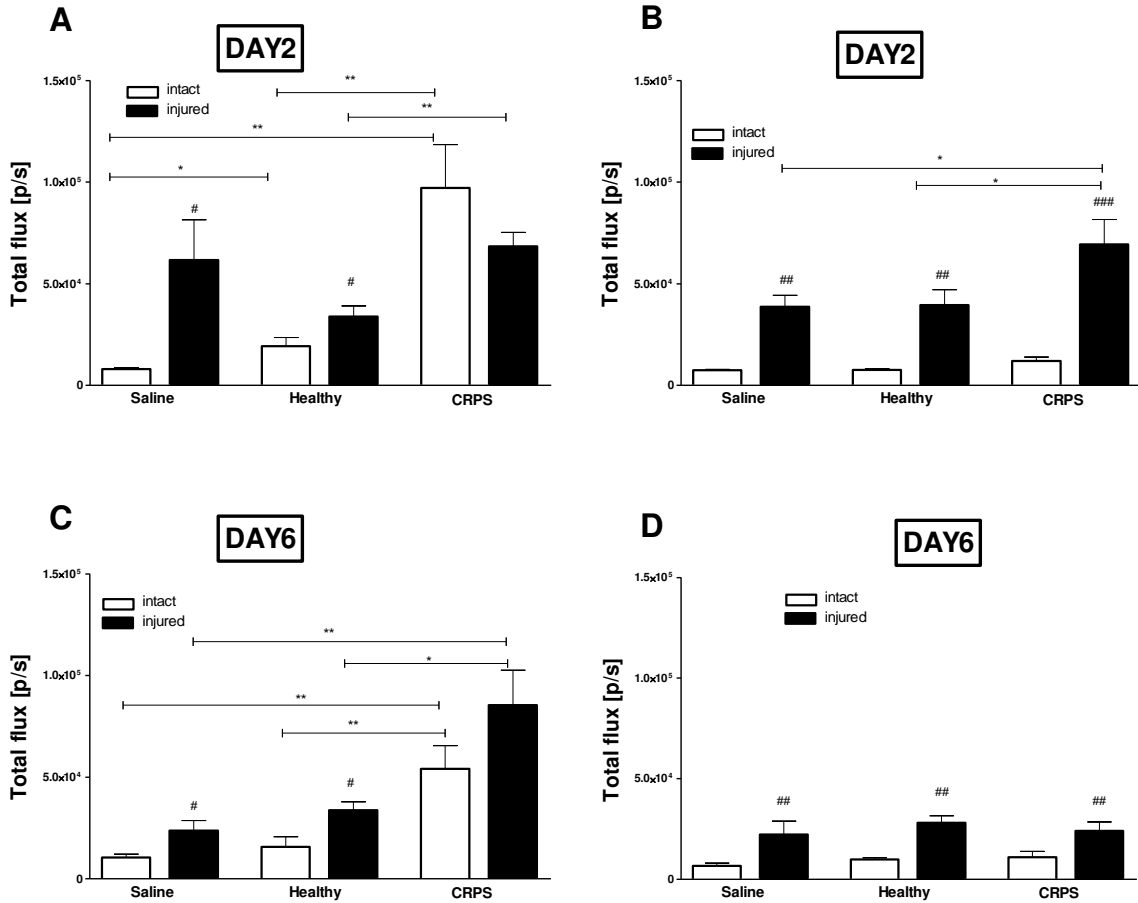
Fig. S4: Data of in vivo images of L-012 - derived bioluminescence for individual patient/healthy preparations on days 2 and 6. Data were obtained from animals treated with various serum-IgG preparations, or saline under general anaesthesia on days 2 and 6 after paw incision. Panel **(A)** shows results from patient #1 on day 2, **(B)** shows pooled results of 2 repeated experiments of patient #3 on day 2. Panels **(C, D)** represent the bioluminescence results of patient #1 and #4 on day 6, respectively. Data are means + SEM, of n= 6-12 mice/group *p < 0.05, **p < 0.01, ***p < 0.001 vs. respective control groups, #p < 0.05, ##p < 0.01, ###p < 0.001 vs. respective intact, one-way ANOVA followed by Bonferroni's multiple comparison test.

Table S2

Day 2	animal number	Day 6	animal number	Day 13	animal number
#1	7	#1	6	#4	6
#3	6	#4	6		
#3	6				
total animal number	19		12		6

**Table S2**. Preparations and animal numbers for in vivo testing (corresponding Figures 4 and S4).

Table S3

Days	1	2	3	5	6	10	13
#2						7^c	
#1					7^c		
#5			6^c				
#3			$6^{b,c}$				
#3	6^c						
#3		6^c					
#3					6^c		
#3		6^c					
#3					$6^{b,c}$		
#3			6^+				
#3			$6^{b,c}$				
#3							$6^{b,c}$
#4			6^c				
#4		6^c					
#4					$6^{b,c}$		
#3			7^+				
#4							$6^{b,c}$
#4	6^c						
#4					5^+		
#4					6^*		
#3					6^*		
#3							$6^{*\,b,c}$
#4					$6\text{-}6^{b,c}$		
#7				6^c			
#6					$6^{b,c}$		
#4 IL-1αβ KO					$6^{b,c}$		
Pooled serum					6^c		
#8 M-IL-1βKO					$4^{b,c}$		
#3 M-IL-1βKO					$4^{b,c}$		

Table S3. List of experiments in the order in which they were done, with animal numbers per group. #1-7=individual patient preparations used; +/* steroid/anakinra experiment; [b] sera were applied for central nervous

system (CNS) immunochemistry, [c] sera were used for behavioural assessment, and evaluation of the mediator levels only (no therapy).
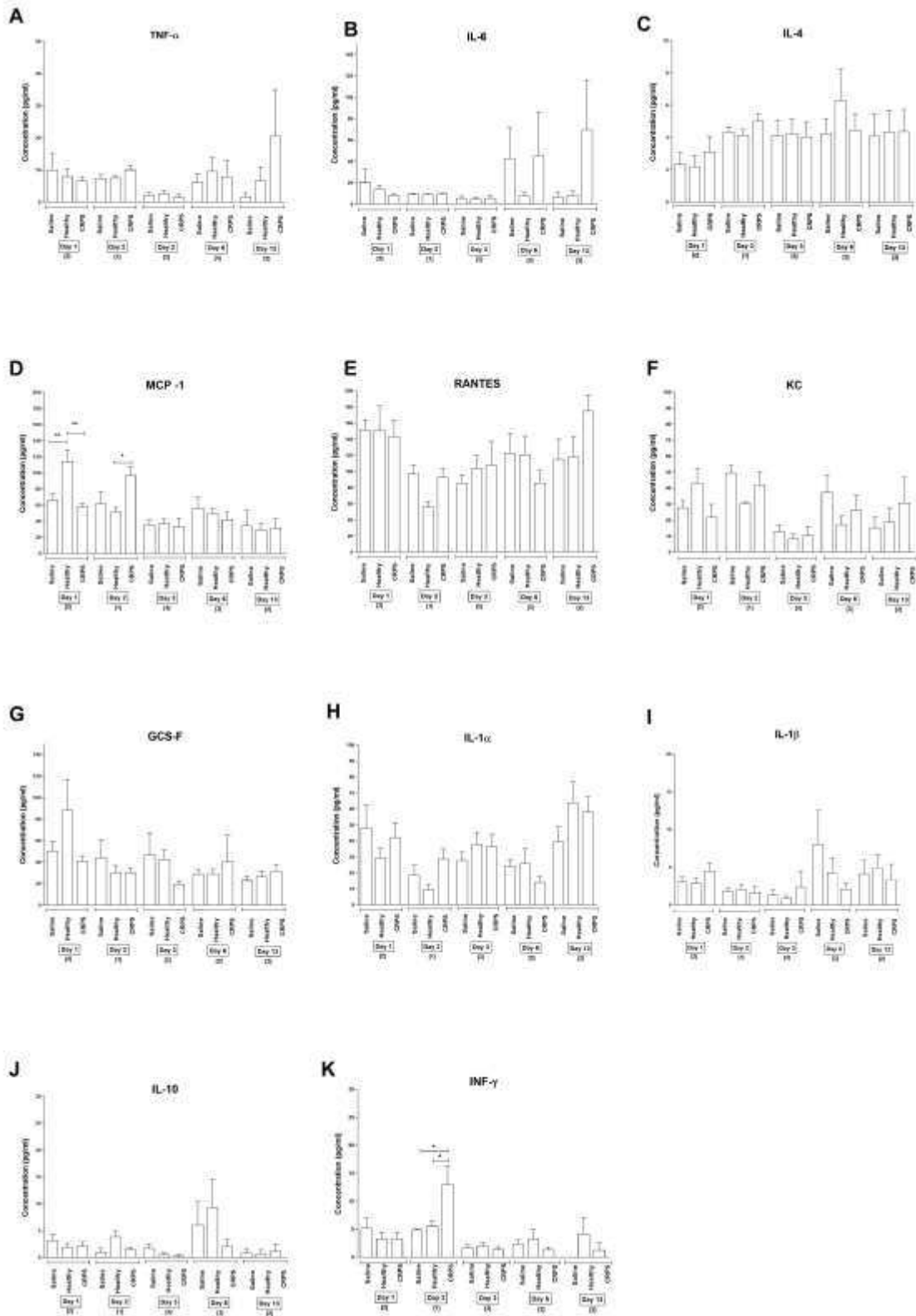
Figure S5
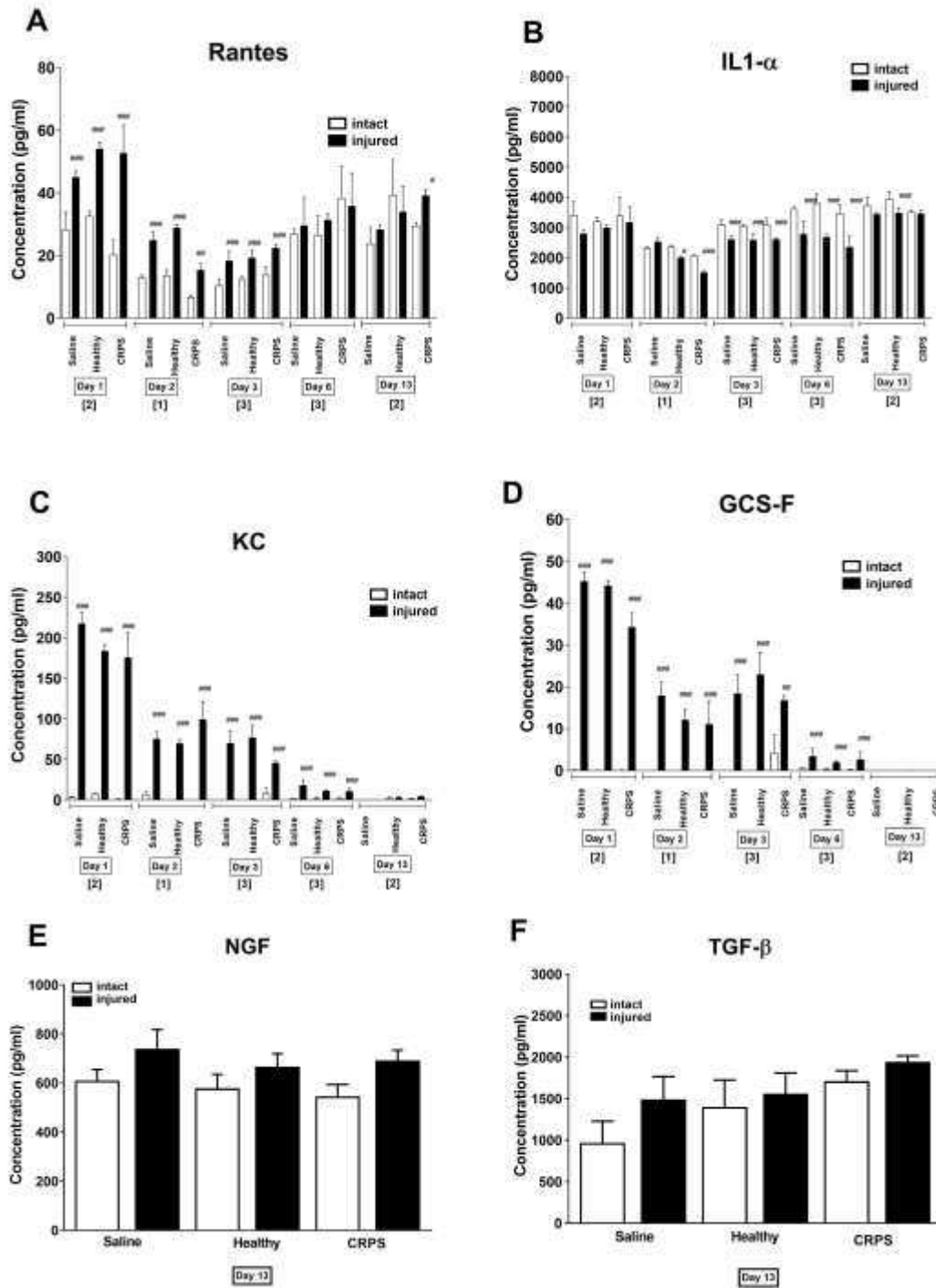
Figure S5 Effects of human IgG treatments and trauma on mediator concentrations in the hindpaws. Concentrations of **(A)** regulated on activation, normal T cell expressed and secreted (Rantes), **(B)** keratinocyte chemoattractant (KC), **(C)** granulocyte-colony stimulating factor (GCS-F), and **(D)** interleukin-1-alpha (IL-1α) were measured by cytometric bead array from the same samples (CBA). Concentrations of **(E)** nerve growth factor (NGF) and **(F)** transforming growth factor beta (TGF-β) were measured by Sandwich ELISA kit.

Levels of interferon-gamma (IFN-γ), interleukin-4 (IL-4) and interleukin-10 (IL-10) were below the detection limit (not shown). Data are from 1-3 experiments with different patient preparations (brackets under the x-axis) per time point, 6 mice/ experiment. The preparations are specified in Table S2. Shown are means $\pm$ SEM; #$p < 0.05$, ##$p < 0.01$, ###$p < 0.001$ vs. respective intact side, one-way ANOVA followed by Bonferroni's multiple comparison test.

Figure S6

Figure S6. Effects of human IgG treatments on mediator concentrations in mouse plasma. Concentrations of **(A)** TNF-α, **(B)** IL-6, **(C)** IL-4, **(D)** MCP-1, (**E**) Rantes, **(F)** KC, **(G)** GCS-F, **(H)** IL-α, **(I)** IL-1β, **(J)** IL-10 and (**K**) IFN-γ were measured by cytometric bead array (CBA) from the same plasma samples. Data are from 1-3 experiments (brackets under x-axis) with different patient preparations per time point, 6 mice/ experiment. Preparations used are specified in Table S4. Shown are means ± SEM; *p < 0.05, **p < 0.01, ***p < 0.001 respective control groups, one-way ANOVA followed by Bonferroni's multiple comparison test. After correction for 10 tests, no significant result remained (not shown).

Figure S7 A
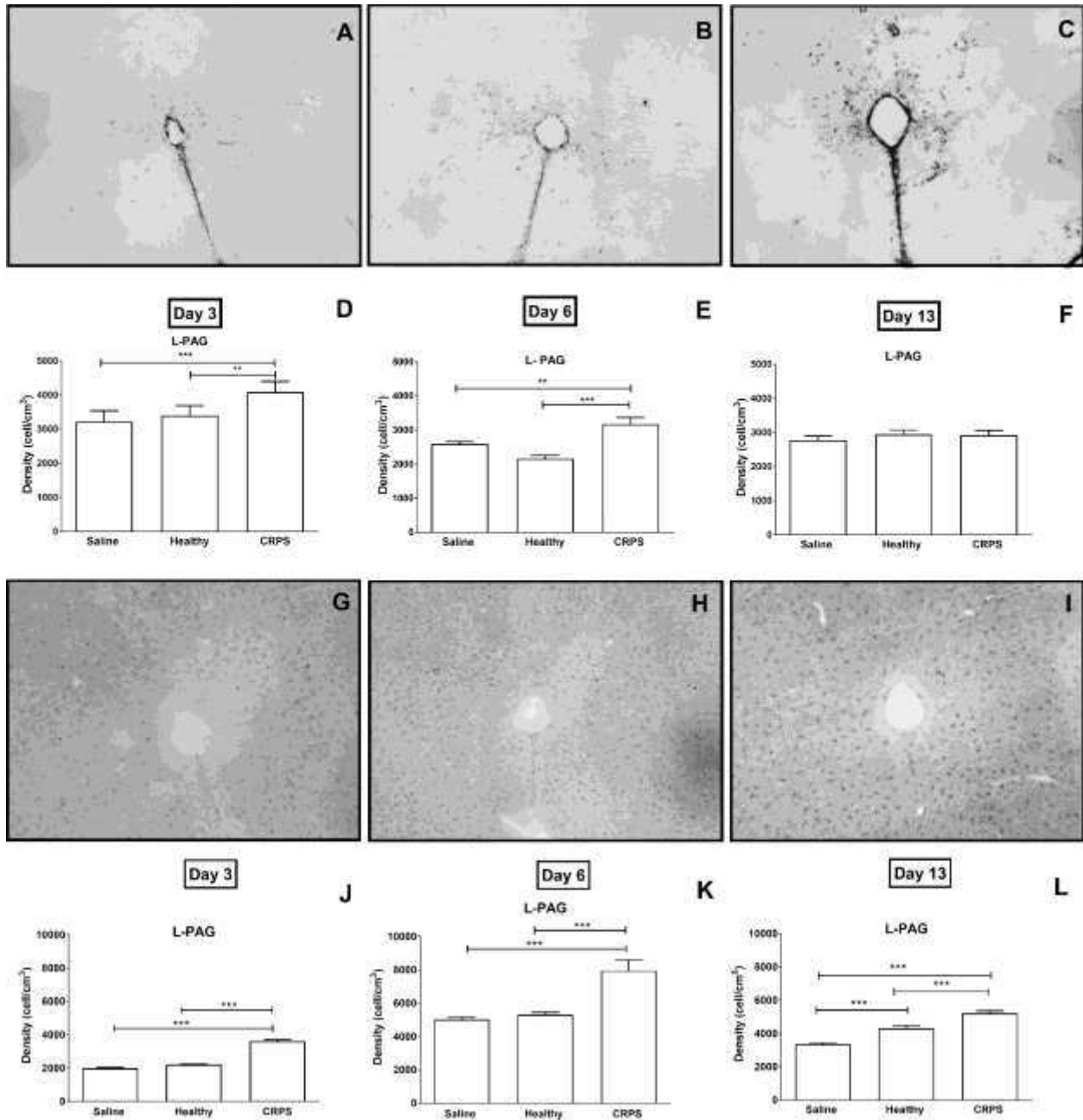
Figure S7A. Representative photomicrographs and quantification of glia cells within the lateral periaqueductal grey matter. Panels **(A-C)** show GFAP immunopositivity indicating astrocytes, and panels **(G-I)** show Iba1 immunopositivity indicating microglia cells ((**A, G**) saline, **(B, H)** healthy, **(C, I)** CRPS groups). The GFAP immunopositive sections shown are from day 6-, and Iba1 sections from day 13 after paw incision. Magnifications are 4x. Panels **(D-F)**: quantification of astrocyte reactivity, and panels **(J-L)** microglia staining at 3, 6, and 13 days post hindpaw incision. Each panel represents the pooled results from 2 experiments with 2 different samples (#3,

#4). Shown are means ± SEM of 6-7 mice per group $*p< 0.05$, $**p< 0.01$, $***p< 0.001$ vs. respective control groups; one-way ANOVA followed by Bonferroni's modified post hoc test.

Figure S7 B
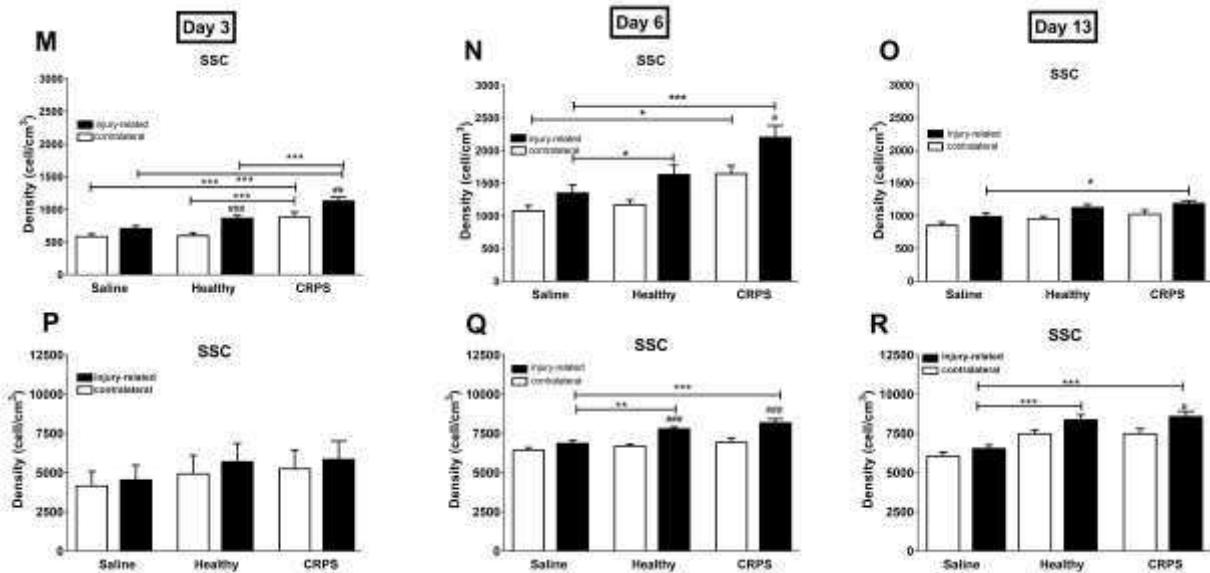
Figure S7B Somatosensory cortex glia cell staining. Quantification of astrocyte reactivity **(M-O)** and microglia staining **(P-R)** in somatosensory cortex ('SSC') at 3, 6, and 13 days post hindpaw incision. Each panel represents the pooled results from 2 experiments with 2 different samples (#3, #4). Shown are means ± SEM o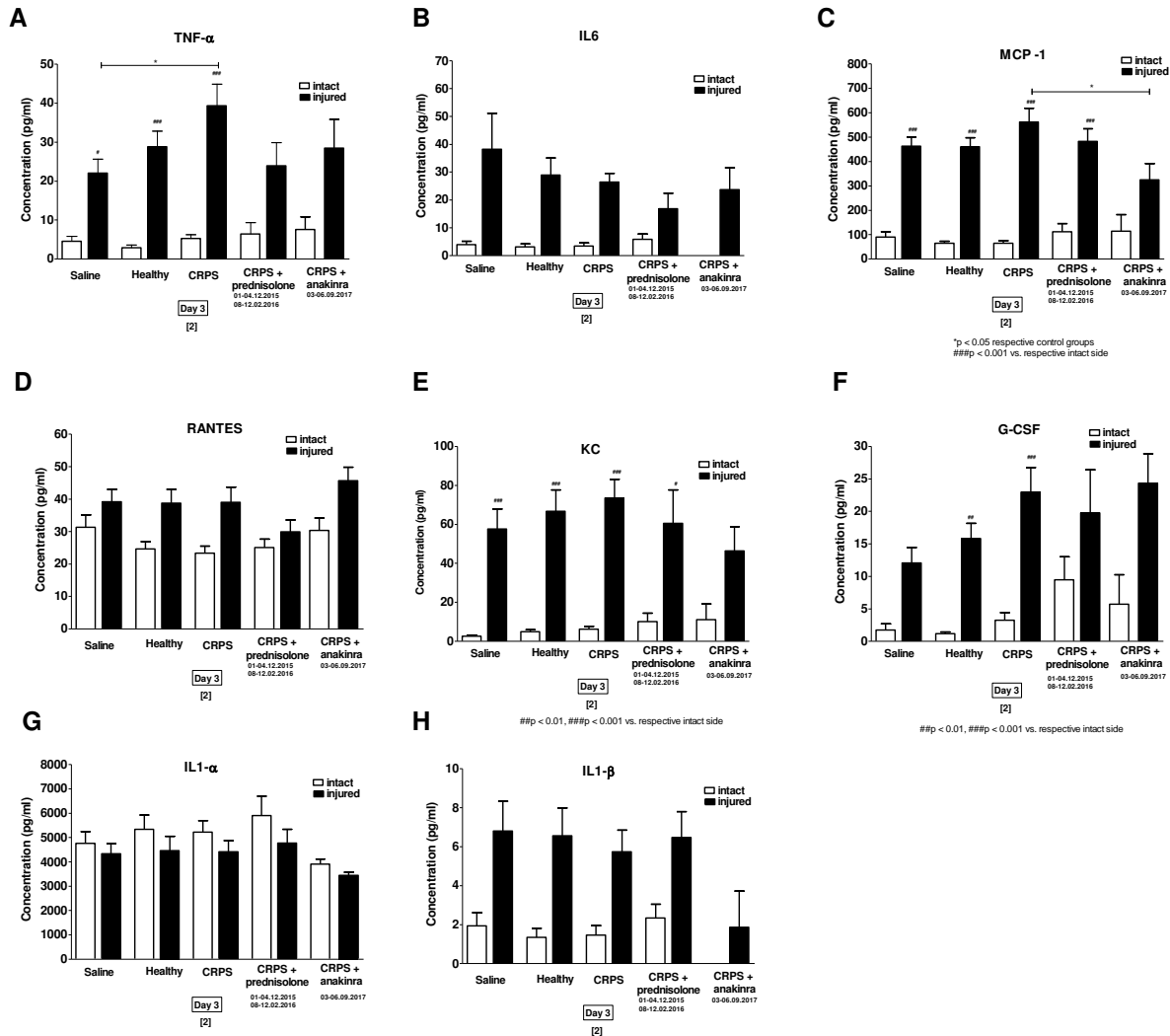f 6-7 mice per group $*p< 0.05$, $**p< 0.01$, $***p< 0.001$ vs. respective control groups; $\#p< 0.05$, $\#\#p< 0.01$, $\#\#\#p< 0.001$ vs. respective contralateral side; one-way ANOVA followed by Bonferroni's modified post hoc test.
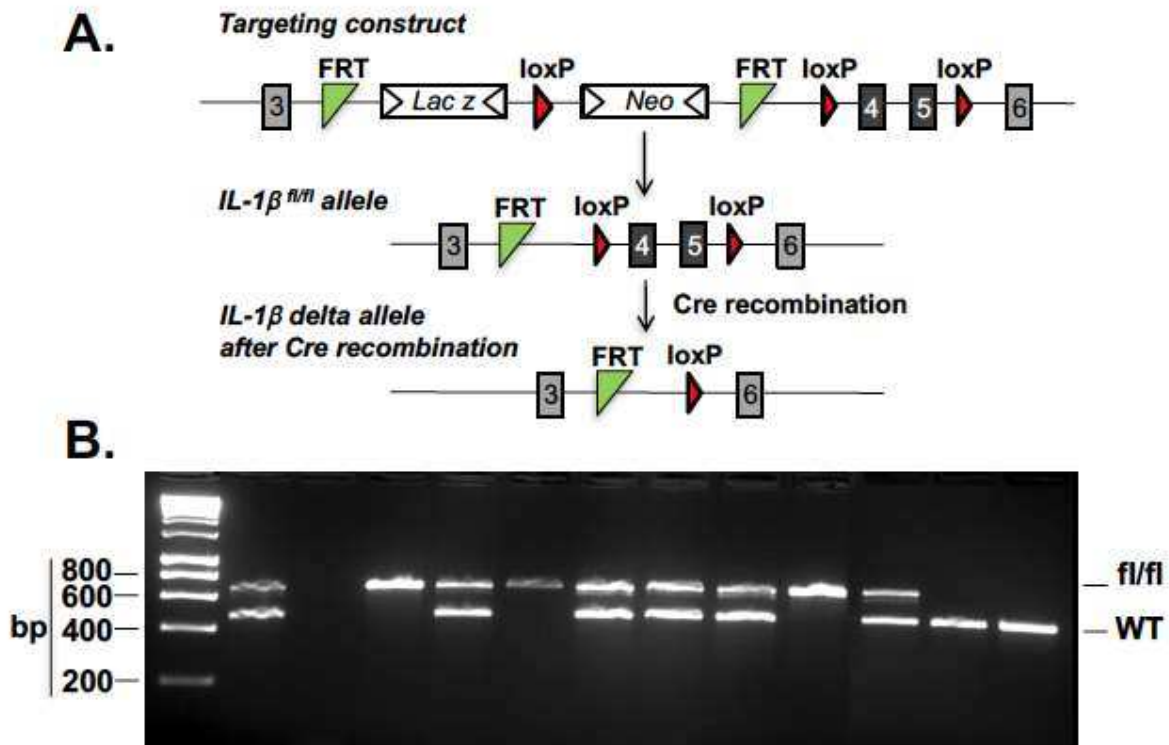
Figure S8

Figure S8. Effects of steroid and anakinra treatment on inflammatory cytokine concentrations in the hindpaws on day 3. (**A**) TNF-α, (**B**) IL-6, (**C**) MCP-1, (**D**) Rantes, (**E**) KC, (**F**) GCS-F, (**G**) IL-1α, (**H**) IL-1β were measured by cytometric bead array (CBA) from the same plasma samples. Other cytokines (IL-4, IL-10 and IFN-γ) were under detection limit. Data are from 2 experiments (brackets under x-axis) with different patient preparations per time point, 6 mice/ experiment (Table S3). Shown are means ± SEM; #$p < 0.05$, ##$p < 0.01$, ###$p < 0.001$ vs. respective intact side, one-way ANOVA followed by Bonferroni's multiple comparison test.

Figure S9

Figure S9. Generation of IL-1b^fl/fl mice. A) Genetic targeting shows exon 4-5 flanked with loxP sites, positioned upstream of a lacZ/Neo resistance cassette, which is excised upon Flp recombination, resulting in the generation of IL-1b^fl/fl allele. Cre recombinase leads to exon 4-5 deletion, generating cell-specific IL-1β KO mice. B) Genotyping PCR showing amplification of the WT (480bp) and IL-1β floxed allele (673bp).

Figure S10

Microglia

CD11b+ spleen cells
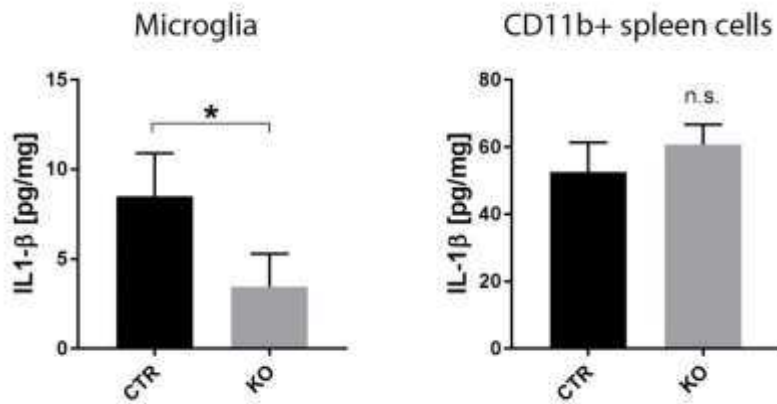
Figure S10. Microglia, but not splenic macrophages derived from tamoxifen-treated Cx3cr1^{CreER} x IL-1β^{fl/fl} mice show elimination of IL-*1β*. Microglia and splenic monocytes/macrophages were isolated by magnetic separation using anti-CD11b microbeads after 12h after priming with intraperitoneal LPS administration, in vivo. IL-1β levels were measured by cytometric bead array and values expressed as pg/mg following correction for protein content. Note that only microglia but not spleen cells show a reduction in IL-1β levels confirming the specific elimination of IL-1β from microglia.

Figure S11
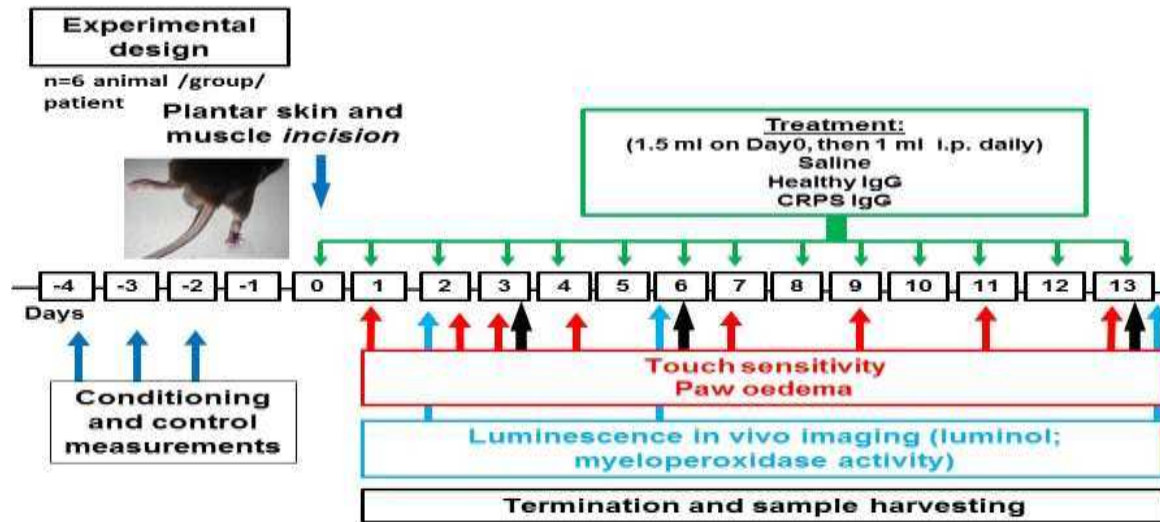
Figure S11. Scheme of the experimental paradigms and investigational techniques. i.p. intraperitoneally; IgG immunoglobulin G, black arrows indicate the time of sample harvesting for central nervous system (CNS) immunochemistry, paws were also harvested on days 1,2, and 10.

Reference list

1. J. Marinus, G. L. Moseley, F. Birklein, R. Baron, C. Maihofner, W. S. Kingery, J. J. van Hilten, Clinical features and pathophysiology of complex regional pain syndrome., Lancet. Neurol. **10**, 637–648 (2011).

2. F. Birklein, S. K. Ajit, A. Goebel, R. S. G. M. Perez, C. Sommer, Complex regional pain syndrome - phenotypic characteristics and potential biomarkers., Nat. Rev. Neurol. **14**, 272–284 (2018).

3. A. Goebel, F. Blaes, Complex regional pain syndrome, prototype of a novel kind of autoimmune disease, Autoimmun. Rev. **12**, 682–686 (2013).

4. C. Maihofner, H. O. Handwerker, B. Neundorfer, F. Birklein, Patterns of cortical reorganization in complex regional pain syndrome., Neurology **61**, 1707–1715 (2003).

5. M. Tajerian, J. D. Clark, New Concepts in Complex Regional Pain Syndrome, Hand Clin. **32**, 41–49 (2016).

6. A. Zyluk, The natural history of post-traumatic reflex sympathetic dystrophy., J. Hand Surg. Br. **23**, 20–23 (1998).

7. M. de Mos, F. J. P. M. Huygen, M. van der Hoeven-Borgman, J. P. Dieleman, B. H. Ch Stricker, M. C. J. M. Sturkenboom, Outcome of the complex regional pain syndrome., Clin. J. Pain **25**, 590–597 (2009).

8. M. A. Kemler, C. A. Furnee, Economic evaluation of spinal cord stimulation for chronic reflex sympathetic dystrophy., Neurology **59**, 1203–1209 (2002).

9. A. Goebel, Complex regional pain syndrome in adults., Rheumatology (Oxford). **50**, 1739–1750 (2011).

10. N. E. O'Connell, B. M. Wand, J. McAuley, L. Marston, G. L. Moseley, Interventions for treating pain and disability in adults with complex regional pain syndrome., Cochrane database Syst. Rev. , CD009416 (2013).

11. S. Barbalinardo, S. A. Loer, A. Goebel, R. S. G. M. Perez, The Treatment of Longstanding Complex Regional Pain Syndrome with Oral Steroids., Pain Med. **17**, 337–343 (2016).

12. A. G. Munts, A. A. van der Plas, M. D. Ferrari, I. M. Teepe-Twiss, J. Marinus, J. J. van Hilten, Efficacy and safety of a single intrathecal methylprednisolone bolus in chronic complex regional pain syndrome., Eur. J. Pain **14**, 523–528 (2010).

13. M. A. Kemler, G. A. Barendse, M. van Kleef, H. C. de Vet, C. P. Rijks, C. A. Furnee, F. A.

van den Wildenberg, Spinal cord stimulation in patients with chronic reflex sympathetic dystrophy., N. Engl. J. Med. **343**, 618–624 (2000).

14. M. A. Kemler, H. C. W. de Vet, G. A. M. Barendse, F. A. J. M. van den Wildenberg, M. van Kleef, Spinal cord stimulation for chronic reflex sympathetic dystrophy--five-year follow-up.N. Engl. J. Med. **354**, 2394–2396 (2006).

15. L. Turner-Stokes, A. Goebel, Complex regional pain syndrome in adults: concise guidance., Clin. Med. **11**, 596–600 (2011).

16. R. Casale, F. Atzeni, P. Sarzi-Puttini, The therapeutic approach to complex regional pain syndrome: light and shade., Clin. Exp. Rheumatol. **33**, S126-39 (2015).

17. R. J. Schwartzman, G. M. Alexander, J. Grothusen, Pathophysiology of complex regional pain syndrome, Expert Rev. Neurother. **6**, 669–681 (2006).

18. V. Tekus, Z. Hajna, É. Borbély, A. Markovics, T. Bagoly, J. Szolcsányi, V. Thompson, Á. Kemény, Z. Helyes, A. Goebel, A CRPS-IgG-transfer-trauma model reproducing inflammatory and positive sensory signs associated with complex regional pain syndrome, Pain **155** (2014), doi:10.1016/j.pain.2013.10.011.

19. E. Aradillas, R. J. Schwartzman, J. R. Grothusen, A. Goebel, G. M. Alexander, Plasma Exchange Therapy in Patients with Complex Regional Pain Syndrome., Pain Physician **18**, 383–394 (2015).

20. A. Goebel, S. Jones, S. Oomman, T. Callaghan, G. Sprotte, Treatment of long-standing complex regional pain syndrome with therapeutic plasma exchange: a preliminary case series of patients treated in 2008-2014.Pain Med. **15**, 2163–2164 (2014).

21. F. J. P. M. Huygen, A. G. J. De Bruijn, M. T. De Bruin, J. G. Groeneweg, J. Klein, F. J. Zijlstra, Evidence for local inflammation in complex regional pain syndrome type 1., Mediators Inflamm. **11**, 47–51 (2002).

22. G. Robinson, H. Cohen, A. Goebel, A case of complex regional pain syndrome with agnosia for object orientation., Pain **152**, 1674–1681 (2011).

23. A. L. Oaklander, J. G. Rissmiller, L. B. Gelman, L. Zheng, Y. Chang, R. Gott, Evidence of focal small-fiber axonal degeneration in complex regional pain syndrome-I (reflex sympathetic dystrophy). (United States, 2006).

24. K. Inoue, M. Tsuda, Microglia in neuropathic pain: cellular and molecular mechanisms and therapeutic potential., Nat. Rev. Neurosci. **19**, 138–152 (2018).

25. Z.-J. Zhang, B.-C. Jiang, Y.-J. Gao, Chemokines in neuron-glial cell interaction and pathogenesis of neuropathic pain. (Switzerland, 2017).

26. K. Popiolek-Barczyk, J. Mika, Targeting the Microglial Signaling Pathways: New Insights in the Modulation of Neuropathic Pain. (United Arab Emirates, 2016).

27. S. M. Allan, P. J. Tyrrell, N. J. Rothwell, Interleukin-1 and neuronal injury., Nat. Rev. Immunol. **5**, 629–640 (2005).

28. A. Denes, E. Pinteaux, N. J. Rothwell, S. M. Allan, Interleukin-1 and stroke: biomarker, harbinger of damage, and therapeutic target., Cerebrovasc. Dis. **32**, 517–527 (2011).

29. S. Yona, K.-W. Kim, Y. Wolf, A. Mildner, D. Varol, M. Breker, D. Strauss-Ayali, S. Viukov, M. Guilliams, A. Misharin, D. A. Hume, H. Perlman, B. Malissen, E. Zelzer, S. Jung, Fate mapping reveals origins and dynamics of monocytes and tissue macrophages under homeostasis. (United States, 2013).

30. R. Fekete, C. Cserep, N. Lenart, K. Toth, B. Orsolits, B. Martinecz, E. Mehes, B. Szabo, V. Nemeth, B. Gonci, B. Sperlagh, Z. Boldogkoi, A. Kittel, M. Baranyi, S. Ferenczi, K. Kovacs, G. Szalay, B. Rozsa, C. Webb, G. G. Kovacs, T. Hortobagyi, B. L. West, Z. Kornyei, A. Denes, Microglia control the spread of neurotropic virus infection via P2Y12 signalling and recruit monocytes through P2Y12-independent mechanisms., Acta Neuropathol. **136**, 461–482 (2018).

31. J. Gierthmuhlen, C. Maier, R. Baron, T. Tolle, R.-D. Treede, N. Birbaumer, V. Huge, J. Koroschetz, E. K. Krumova, M. Lauchart, C. Maihofner, H. Richter, A. Westermann, Sensory signs in complex regional pain syndrome and peripheral nerve injury., Pain **153**, 765–774 (2012).

32. A. Goebel, Autoantibody pain, Autoimmun. Rev. **15**, 552–557 (2016).

33. G. Wigerblad, D. B. Bas, C. Fernades-Cerqueira, A. Krishnamurthy, K. S. Nandakumar, K. Rogoz, J. Kato, K. Sandor, J. Su, J. M. Jimenez-Andrade, A. Finn, A. Bersellini Farinotti, K. Amara, K. Lundberg, R. Holmdahl, P.-J. Jakobsson, V. Malmstrom, A. I. Catrina, L. Klareskog, C. I. Svensson, Autoantibodies to citrullinated proteins induce joint pain independent of inflammation via a chemokine-dependent mechanism., Ann. Rheum. Dis. **75**, 730–738 (2016).

34. F. Blaes, K. Schmitz, M. Tschernatsch, M. Kaps, I. Krasenbrink, G. Hempelmann, M. E. Brau, Autoimmune etiology of complex regional pain syndrome (M. Sudeck)., Neurology **63**, 1734–1736 (2004).

35. E. Dubuis, V. Thompson, M. I. Leite, F. Blaes, C. Maihofner, D. Greensmith, A. Vincent, N.

Shenker, A. Kuttikat, M. Leuwer, A. Goebel, Longstanding complex regional pain syndrome is associated with activating autoantibodies against alpha-1a adrenoceptors., Pain **155**, 2408–2417 (2014).

36. R. J. M. Munnikes, C. Muis, M. Boersma, C. Heijmans-Antonissen, F. J. Zijlstra, F. J. P. M. Huygen, Intermediate stage complex regional pain syndrome type 1 is unrelated to proinflammatory cytokines., Mediators Inflamm. **2005**, 366–372 (2005).

37. F. Birklein, T. Schlereth, Complex regional pain syndrome-significant progress in understanding., Pain **156 Suppl**, S94-103 (2015).

38. P. H. Veldman, H. M. Reynen, I. E. Arntz, R. J. Goris, Signs and symptoms of reflex sympathetic dystrophy: prospective study of 829 patients., Lancet (London, England) **342**, 1012–1016 (1993).

39. M. R. Suter, Microglial role in the development of chronic pain. (United States, 2016).

40. E. D. Milligan, L. R. Watkins, Pathological and protective roles of glia in chronic pain. (England, 2009).

41. K. Christensen, E. M. Jensen, I. Noer, The reflex dystrophy syndrome response to treatment with systemic corticosteroids., Acta Chir. Scand. **148**, 653–655 (1982).

42. C.-Y. Chiang, B. J. Sessle, J. O. Dostrovsky, Role of astrocytes in pain., Neurochem. Res. **37**, 2419–2431 (2012).

43. W. Guo, H. Wang, M. Watanabe, K. Shimizu, S. Zou, S. C. LaGraize, F. Wei, R. Dubner, K. Ren, Glial—Cytokine—Neuronal Interactions Underlying the Mechanisms of Persistent Pain, J. Neurosci. **27**, 6006–6018 (2007).

44. J. M. Pradillo, A. Denes, A. D. Greenhalgh, H. Boutin, C. Drake, B. W. McColl, E. Barton, S. D. Proctor, J. C. Russell, N. J. Rothwell, S. M. Allan, Delayed administration of interleukin-1 receptor antagonist reduces ischemic brain damage and inflammation in comorbid rats., J. Cereb. Blood Flow Metab. **32**, 1810–1819 (2012).

45. A. Denes, P. Thornton, N. J. Rothwell, S. M. Allan, Inflammation and brain injury: acute cerebral ischaemia, peripheral and central inflammation., Brain. Behav. Immun. **24**, 708–723 (2010).

46. A. Denes, C. Drake, J. Stordy, J. Chamberlain, B. W. McColl, H. Gram, D. Crossman, S. Francis, S. M. Allan, N. J. Rothwell, Interleukin-1 mediates neuroinflammatory changes associated with diet-induced atherosclerosis., J. Am. Heart Assoc. **1**, e002006 (2012).

47. A. Denes, J. M. Pradillo, C. Drake, A. Sharp, P. Warn, K. N. Murray, B. Rohit, D. H. Dockrell, J. Chamberlain, H. Casbolt, S. Francis, B. Martinecz, B. Nieswandt, N. J. Rothwell, S. M. Allan, Streptococcus pneumoniae worsens cerebral ischemia via interleukin 1 and platelet glycoprotein Ibalpha., Ann. Neurol. **75**, 670–683 (2014).

48. S. A. Liddelow, K. A. Guttenplan, L. E. Clarke, F. C. Bennett, C. J. Bohlen, L. Schirmer, M. L. Bennett, A. E. Munch, W.-S. Chung, T. C. Peterson, D. K. Wilton, A. Frouin, B. A. Napier, N. Panicker, M. Kumar, M. S. Buckwalter, D. H. Rowitch, V. L. Dawson, T. M. Dawson, B. Stevens, B. A. Barres, Neurotoxic reactive astrocytes are induced by activated microglia., Nature **541**, 481–487 (2017).

49. W. Liu, Y. Tang, J. Feng, Cross talk between activation of microglia and astrocytes in pathological conditions in the central nervous system., Life Sci. **89**, 141–146 (2011).

50. K. V Toyka, D. B. Brachman, A. Pestronk, I. Kao, Myasthenia gravis: passive transfer from man to mouse., Science **190**, 397–399 (1975).

51. P. Sillevis Smitt, A. Kinoshita, B. De Leeuw, W. Moll, M. Coesmans, D. Jaarsma, S. Henzen-Logmans, C. Vecht, C. De Zeeuw, N. Sekiyama, S. Nakanishi, R. Shigemoto, Paraneoplastic cerebellar ataxia due to autoantibodies against a glutamate receptor., N. Engl. J. Med. **342**, 21–27 (2000).

52. J. Schwartz, A. Padmanabhan, N. Aqui, R. A. Balogun, L. Connelly-Smith, M. Delaney, N. M. Dunbar, V. Witt, Y. Wu, B. H. Shaz, Guidelines on the Use of Therapeutic Apheresis in Clinical Practice-Evidence-Based Approach from the Writing Committee of the American Society for Apheresis: The Seventh Special Issue., J. Clin. Apher. **31**, 149–162 (2016).

53. G. Lopalco, D. Rigante, M. Giannini, M. Galeazzi, G. Lapadula, F. Iannone, L. Cantarini, Safety profile of anakinra in the management of rheumatologic, metabolic and autoinflammatory disorders., Clin. Exp. Rheumatol. **34**, 531–538 (2016).

54. M. T. Nurmohamed, B. A. C. Dijkmans, Efficacy, tolerability and cost effectiveness of disease-modifying antirheumatic drugs and biologic agents in rheumatoid arthritis., Drugs **65**, 661–694 (2005).

55. P. B. Petersen, K. L. Mikkelsen, J. B. Lauritzen, M. R. Krogsgaard, Risk factors for post-treatment complex regional pain syndrome (CRPS) - an analysis of 647 cases of CRPS from the Danish Patient Compensation Association., Pain Pract. (2017), doi:10.1111/papr.12610.

56. V. W. Jaenig W., Schaumann R., CRPS (Complex Regional Pain Syndrome)SUVA (2013)

(available at https://www.suva.ch/material/dokumentationen/crps-complex-regional-pain-syndrome-2771.d-12683-12683).

57. N. P. Staff, J. Engelstad, C. J. Klein, K. K. Amrami, R. J. Spinner, P. J. Dyck, M. A. Warner, M. E. Warner, P. J. B. Dyck, Post-surgical inflammatory neuropathy. (England, 2010).

58. A. Goebel, A. Jacob, B. Frank, P. Sacco, G. Alexander, C. Philips, P. Bassett, R. Moots, Mycophenolate for persistent complex regional pain syndrome, a parallel, open, randomised, proof of concept trial., Scand. J. pain **18**, 29–37 (2018).

59. G. L. Moseley, R. D. Herbert, T. Parsons, S. Lucas, J. J. Van Hilten, J. Marinus, Intense pain soon after wrist fracture strongly predicts who will develop complex regional pain syndrome: prospective cohort study. (United States, 2014).

60. E. M. Pogatzki, S. N. Raja, A Mouse Model of Incisional Pain Materials and Methods, Anesthesiology **99**, 1023–7 (2003).

61. J. R. Clapper, G. Moreno-Sanz, R. Russo, A. Guijarro, F. Vacondio, A. Duranti, A. Tontini, S. Sanchini, N. R. Sciolino, J. M. Spradley, A. G. Hohmann, A. Calignano, M. Mor, G. Tarzia, D. Piomelli, Anandamide suppresses pain initiation through a peripheral endocannabinoid mechanism., Nat. Neurosci. **13**, 1265–1270 (2010).

62. S. Venteo, S. Laffray, C. Wetzel, C. Rivat, F. Scamps, I. Mechaly, L. Bauchet, C. Raoul, E. Bourinet, G. R. Lewin, P. Carroll, A. Pattyn, Fxyd2 regulates Adelta- and C-fiber mechanosensitivity and is required for the maintenance of neuropathic pain., Sci. Rep. **6**, 36407 (2016).

63. K. Bölcskei, Z. Helyes, Á. Szabó, K. Sándor, K. Elekes, J. Németh, R. Almási, E. Pintér, G. Petho, J. Szolcsányi, Investigation of the role of TRPV1 receptors in acute and chronic nociceptive processes using gene-deficient mice, Pain **117**, 368–376 (2005).

64. B. Costa, F. Comelli, I. Bettoni, M. Colleoni, G. Giagnoni, The endogenous fatty acid amide, palmitoylethanolamide, has anti-allodynic and anti-hyperalgesic effects in a murine model of neuropathic pain: involvement of CB1, TRPV1 and PPAR?? receptors and neurotrophic factors, Pain **139**, 541–550 (2008).

65. Á. Szabó, Z. Helyes, K. Sándor, A. Bite, E. Pintér, J. Németh, Á. Bánvölgyi, K. Bölcskei, K. Elekes, J. Szolcsányi, Role of Transient Receptor Potential Vanilloid 1 Receptors in Adjuvant-Induced Chronic Arthritis: In Vivo Study Using Gene-Deficient Mice, J. Pharmacol. Exp. Ther. **314**, 111 LP-119 (2005).

66. L. Negri, R. Lattanzi, E. Giannini, M. Colucci, F. Margheriti, P. Melchiorri, V. Vellani, H. Tian, M. De Felice, F. Porreca, Impaired Nociception and Inflammatory Pain Sensation in Mice Lacking the Prokineticin Receptor PKR1: Focus on Interaction between PKR1 and the Capsaicin Receptor TRPV1 in Pain Behavior, J. Neurosci. **26**, 6716 LP-6727 (2006).

67. A.-K. Kirchherr, A. Briel, K. Mader, Stabilization of indocyanine green by encapsulation within micellar systems., Mol. Pharm. **6**, 480–491 (2009).

68. Horváth, V. Tékus, M. Boros, G. Pozsgai, B. Botz, Borbély, J. Szolcsányi, E. Pintér, Z. Helyes, Transient receptor potential ankyrin 1 (TRPA1) receptor is involved in chronic arthritis: In vivo study using TRPA1-deficient mice, Arthritis Res. Ther. **18** (2016), doi:10.1186/s13075-015-0904-y.

69. Y. Nishinaka, Y. Aramaki, H. Yoshida, H. Masuya, T. Sugawara, Y. Ichimori, A New Sensitive Chemiluminescence Probe, L-012, for Measuring the Production of Superoxide Anion by Cells, Biochem. Biophys. Res. Commun. **193**, 554–559 (1993).

70. A. Kielland, T. Blom, K. S. Nandakumar, R. Holmdahl, R. Blomhoff, H. Carlsen, In vivo imaging of reactive oxygen and nitrogen species in inflammation using the luminescent probe L-012, Free Radic. Biol. Med. **47**, 760–766 (2009).

71. A. Daiber, M. Oelze, M. August, M. Wendt, K. Sydow, H. Wieboldt, A. L. Kleschyov, T. Munzel, Detection of superoxide and peroxynitrite in model systems and mitochondria by the luminol analogue L-012., Free Radic. Res. **38**, 259–269 (2004).

72. I. Imada, E. F. Sato, M. Miyamoto, Y. Ichimori, Y. Minamiyama, R. Konaka, M. Inoue, Analysis of Reactive Oxygen Species Generated by Neutrophils Using a Chemiluminescence Probe L-012, Anal. Biochem. **271**, 53–58 (1999).

73. B. Botz, K. Bölcskei, L. Kereskai, M. Kovács, T. Németh, K. Szigeti, I. Horváth, D. Máthé, N. Kovács, H. Hashimoto, D. Reglődi, J. Szolcsányi, E. Pintér, A. Mócsai, Z. Helyes, Differential Regulatory Role of Pituitary Adenylate Cyclase–Activating Polypeptide in the Serum-Transfer Arthritis Model, Arthritis Rheumatol. (Hoboken, N.j.) **66**, 2739–2750 (2014).

74. J.-C. Tseng, A. L. Kung, In Vivo Imaging of Inflammatory Phagocytes, Chem. Biol. **19**, 1199–1209 (2012).

75. M. Weber, F. Birklein, B. Neundorfer, M. Schmelz, Facilitated neurogenic inflammation in complex regional pain syndrome., Pain **91**, 251–257 (2001).

76. J. Nemeth, G. Oroszi, M. Than, Z. S. Helyes, E. Pinter, B. Farkas, J. Szolcsanyi, Substance P

radioimmunoassay for quantitative characterization of sensory neurotransmitter release., Neurobiology (Bp). **7**, 437–444 (1999).

77. J. Nemeth, T. Gorcs, Z. Helyes, G. Oroszi, T. Kocsy, E. Pinter, J. Szolcsanyi, Development of a new sensitive CGRP radioimmunoassay for neuropharmacological research., Neurobiology (Bp). **6**, 473–475 (1998).

78. A. Denes, G. Coutts, N. Lénárt, S. M. Cruickshank, P. Pelegrin, J. Skinner, N. Rothwell, S. M. Allan, D. Brough, AIM2 and NLRC4 inflammasomes contribute with ASC to acute brain injury independently of NLRP3, Proc. Natl. Acad. Sci. U. S. A. **112**, 4050–4055 (2015).

79. J. B. Davis, ELISA for Monitoring Nerve Growth Factor., Methods Mol. Biol. **1606**, 141–147 (2017).

80. M. G. Giovannini, R. D. Blitzer, T. Wong, K. Asoma, P. Tsokas, J. H. Morrison, R. Iyengar, E. M. Landau, Mitogen-activated protein kinase regulates early phosphorylation and delayed expression of Ca2+/calmodulin-dependent protein kinase II in long-term potentiation., J. Neurosci. **21**, 7053–7062 (2001).

81. F. Cerbai, D. Lana, D. Nosi, P. Petkova-Kirova, S. Zecchi, H. M. Brothers, G. L. Wenk, M. G. Giovannini, C. M. Norris, Ed. The Neuron-Astrocyte-Microglia Triad in Normal Brain Ageing and in a Model of Neuroinflammation in the Rat Hippocampus, PLoS One **7**, e45250 (2012).

82. R. L. Stornetta, C. P. Sevigny, P. G. Guyenet, Vesicular glutamate transporter DNPI/VGLUT2 mRNA is present in C1 and several other groups of brainstem catecholaminergic neurons., J. Comp. Neurol. **444**, 191–206 (2002).

83. M. D. C. Valdes Hernandez, P. J. Gallacher, M. E. Bastin, N. A. Royle, S. M. Maniega, I. J. Deary, J. M. Wardlaw, Automatic segmentation of brain white matter and white matter lesions in normal aging: comparison of five multispectral techniques., Magn. Reson. Imaging **30**, 222–229 (2012).

84. M. M. Petrinovic, G. Hankov, A. Schroeter, A. Bruns, M. Rudin, M. von Kienlin, B. Kunnecke, T. Mueggler, A novel anesthesia regime enables neurofunctional studies and imaging genetics across mouse strains., Sci. Rep. **6**, 24523 (2016).

85. G. Paxinos, K. Franklin, *Paxinos and Franklin's the Mouse* Brain in Stereotaxic Coordinates (2012; https://www.elsevier.com/books/paxinos-and-franklins-the-mouse-brain-in-stereotaxic-coordinates/paxinos/978-0-12-391057-8).

86. Z. Varga, D. Csabai, A. Miseta, O. Wiborg, B. Czeh, Chronic stress affects the number of GABAergic neurons in the orbitofrontal cortex of rats., Behav. Brain Res. **316**, 104–114 (2017).

87. L. He, N. Uceyler, H. H. Kramer, M. N. Colaco, B. Lu, F. Birklein, C. Sommer, Methylprednisolone prevents nerve injury-induced hyperalgesia in neprilysin knockout mice., Pain **155**, 574–580 (2014).

88. M. Suzuki, H. Yoshida, M. Hashizume, K. Tanaka, Y. Matsumoto, Blockade of interleukin-6 receptor enhances the anti-arthritic effect of glucocorticoids without decreasing bone mineral density in mice with collagen-induced arthritis., Clin. Exp. Immunol. **182**, 154–161 (2015).

89. R. G. Iannitti, V. Napolioni, V. Oikonomou, A. De Luca, C. Galosi, M. Pariano, C. Massi-Benedetti, M. Borghi, M. Puccetti, V. Lucidi, C. Colombo, E. Fiscarelli, C. Lass-Florl, F. Majo, L. Cariani, M. Russo, L. Porcaro, G. Ricciotti, H. Ellemunter, L. Ratclif, F. M. De Benedictis, V. N. Talesa, C. A. Dinarello, F. L. van de Veerdonk, L. Romani, IL-1 receptor antagonist ameliorates inflammasome-dependent inflammation in murine and human cystic fibrosis., Nat. Commun. **7**, 10791 (2016).

90. M. Gertsenstein, L. M. J. Nutter, T. Reid, M. Pereira, W. L. Stanford, J. Rossant, A. Nagy, Efficient generation of germ line transmitting chimeras from C57BL/6N ES cells by aggregation with outbred host embryos., PLoS One **5**, e11260 (2010).

91. W. C. Skarnes, B. Rosen, A. P. West, M. Koutsourakis, W. Bushell, V. Iyer, A. O. Mujica, M. Thomas, J. Harrow, T. Cox, D. Jackson, J. Severin, P. Biggs, J. Fu, M. Nefedov, P. J. de Jong, A. F. Stewart, A. Bradley, A conditional knockout resource for the genome-wide study of mouse gene function., Nature **474**, 337–342 (2011).

Bibliography

1. Staff NP, Engelstad J, Klein CJ, Amrami KK, Spinner RJ, Dyck PJ, et al. Post-surgical inflammatory neuropathy. Brain. 2010;133(10):2866-80.

2. Goebel A, Jacob A, Frank B, Sacco P, Alexander G, Philips C, et al. Mycophenolate for persistent complex regional pain syndrome, a parallel, open, randomised, proof of concept trial. Scandinavian Journal of Pain. 2018;18(1):29-37.